Research Paper

PAIN®

OPEN

ACVR1-activating mutation causes neuropathic pain and sensory neuron hyperexcitability in humans

Xiaobing Yu[a,*], Amy N. Ton[b], Zejun Niu[a,c], Blanca M. Morales[b], Jiadong Chen[d], Joao Braz[e], Michael H. Lai[f], Emilie Barruet[b], Hongju Liu[a,g], Kin Cheung[h], Syed Ali[a], Tea Chan[b], Katherine Bigay[b], Jennifer Ho[b], Ina Nikolli[b], Steven Hansberry[b,i], Kelly Wentworth[b], Arnold Kriegstein[d], Allan Basbaum[e], Edward C. Hsiao[b]

Abstract

Altered bone morphogenetic protein (BMP) signaling is associated with many musculoskeletal diseases. However, it remains unknown whether BMP dysfunction has direct contribution to debilitating pain reported in many of these disorders. Here, we identified a novel neuropathic pain phenotype in patients with fibrodysplasia ossificans progressiva (FOP), a rare autosomal-dominant musculoskeletal disorder characterized by progressive heterotopic ossification. Ninety-seven percent of these patients carry an R206H gain-of-function point mutation in the BMP type I receptor ACVR1 (ACVR1^{R206H}), which causes neofunction to Activin A and constitutively activates signaling through phosphorylated SMAD1/5/8. Although patients with FOP can harbor pathological lesions in the peripheral and central nervous system, their etiology and clinical impact are unclear. Quantitative sensory testing of patients with FOP revealed significant heat and mechanical pain hypersensitivity. Although there was no major effect of ACVR1^{R206H} on differentiation and maturation of nociceptive sensory neurons (iSNs) derived from FOP induced pluripotent stem cells, both intracellular and extracellular electrophysiology analyses of the ACVR1^{R206H} iSNs displayed ACVR1-dependent hyperexcitability, a hallmark of neuropathic pain. Consistent with this phenotype, we recorded enhanced responses of ACVR1^{R206H} iSNs to TRPV1 and TRPA1 agonists. Thus, activated ACVR1 signaling can modulate pain processing in humans and may represent a potential target for pain management in FOP and related BMP pathway diseases.

Keywords: ACVR1, Fibrodysplasia ossificans progressiva, FOP, BMP, Induced pluripotent stem cells, iPSC, Nociceptor, iSN, Sensory neuron, DRG, TRPV1, TRPA1, Quantitative sensory testing, QST, Neuropathic pain, MEA

1. Introduction

Fibrodysplasia ossificans progressiva (FOP) is a rare autosomal-dominant musculoskeletal disorder characterized by progressive heterotopic ossification (HO) of muscle, fascia, ligaments, and tendons,[54] which results in progressive disability and significant comorbidities. Approximately 97% of patients with FOP carry an arginine[206] to histidine gain-of-function point mutation in the intracellular domain of the BMP type I receptor ACVR1 (ACVR1^{R206H}).[54] This mutation activates intracellular signaling through phosphorylated SMAD1/5/8 (pSMAD1/5/8)[64] and also misinterprets Activin A as a BMP ligand, resulting in abnormal BMP-like signaling.[22] In addition to the dramatic HO, pathological changes in the peripheral and central nervous system[33] appear in a number of patients with FOP[28,35,76] but with unclear etiology or clinical significance. Separately, the recent discovery that 25% of the patients who suffer from diffuse intrinsic pontine glioma[7,18,69] also carry gain-of-function ACVR1 mutations, including ACVR1^{R206H}, suggests that dysregulated ACVR1 activity is involved in a number of neurological disorders.[19,26] However, the mechanisms through which ACVR1 variants contribute to neuronal dysfunction are unclear.

Debilitating pain is a particularly significant clinical challenge for patients with FOP. Chronic pain was reported by 86% of patients in one cohort,[53] and 23 to 31% of patients reported hypersensitivity to touch or abnormal temperature sensation at baseline.[35] Despite pain being a prominent symptom of FOP, the exact

Sponsorships or competing interests that may be relevant to content are disclosed at the end of this article.

Xiaobing Yu, Amy N. Ton, Zejun Niu, and Blanca M. Morales contributed equally to this work.

[a] Department of Anesthesia and Perioperative Care, University of California San Francisco, San Francisco, CA, United States, [b] Division of Endocrinology and Metabolism, Department of Medicine, The Institute for Human Genetics, and the Program in Craniofacial Biology, University of California, San Francisco, CA, United States, [c] Department of Anesthesiology, the Affiliated Hospital of Qingdao University, Qingdao, China, [d] Department of Neurology, University of California, San Francisco, CA, United States. Dr. Chen is now with the Department of Neurology of Second Affiliated Hospital, Centre for Neuroscience, Zhejiang University School of Medicine, Hangzhou, China, [e] Department of Anatomy, University of California San Francisco, San Francisco, CA, United States, [f] J. David Gladstone Institutes, San Francisco, CA, United States, [g] Department of Anesthesiology, Peking Union Medical College Hospital, Beijing, China, [h] BioSAS Consulting, Inc, Wellesley, MA, United States, [i] California Institute of Regenerative Medicine Bridges to Stem Cell Research Program, San Francisco State University, San Francisco, CA, United States

**Corresponding author. Address: Department of Anesthesia and Perioperative Care School of Medicine University of California, San Francisco 533 Parnassus Avenue UC Hall Room 368N San Francisco, CA 94143 United States. Tel.: +1 415 514-3781. E-mail address: Xiaobing.Yu@ucsf.edu (X. Yu).*

Supplemental digital content is available for this article. Direct URL citations appear in the printed text and are provided in the HTML and PDF versions of this article on the journal's Web site (www.painjournalonline.com).

PAIN 164 (2023) 43–58

http://dx.doi.org/10.1097/j.pain.0000000000002656

nature and mechanism remain unclear. To define the potential baseline sensory dysfunction in patients with FOP, here, we analyzed the data from the International FOP Association (IFOPA) Connection Registry[43] and observed that patients with FOP have a high incidence of symptoms of neuropathic pain. Specifically, quantitative sensory testing (QST) on a cohort of patients carrying the classical ACVR1^{R206H} mutation revealed increased pain sensitivity to both mechanical and heat noxious stimuli.

Nociception in the existing preclinical FOP mouse models has not been studied to date, partly because the neurologic phenotypes in FOP remain poorly understood. Although there is a growing translatability advantage to model chronic pain using human tissues,[6,48,52,78] primary human neuronal tissue is limited in availability and particularly difficult to obtain in the FOP patient population because invasive procedures including surgery and biopsy can trigger massive HO.[54] Therefore, we used human induced pluripotent stem cell (iPSC)-derived nociceptive sensory neurons (iSNs) which provide us a unique opportunity to elucidate how pain transmission is altered chronically and identify potential peripheral therapeutic targets[10,13,46,73] in patients with FOP.

Compared with healthy controls, FOP iPSC-derived ACVR1^{R206H} iSNs showed hyperexcitability and increased susceptibility to stimulation by either TRPV1 or TRPA1 agonists, independent from interpatient genetic or clonal variability. Finally, blocking the constitutively active ACVR1 signaling in FOP iSNs leads to a significant reduction in neuronal firings, further suggesting that ACVR1-mediated sensory neuron dysfunction contributes to the baseline neuropathic pain in FOP.

2. Materials and methods

2.1. The Fibrodysplasia Ossificans Progressiva Connection Registry and statistical analyses

The survey design and implementation of the FOP Connection Registry, including a description of the human subjects' protection protocols, have been previously published.[43] For continuous variables, mean, median, SD, minimum, and maximum were calculated. Percentages were based on all participants enrolled within each category and age group. Participants with duplicate assessments or who withdrew from the registry were excluded. To test the association between patients with FOP with and without neuropathic pain, we performed a Wilcoxon rank-sum test on PROMIS Total Quality of Life Score, PFQ, Aides, and Assistive Devices. Details of specific devices that were queried in the survey are listed in Table S1, http://links.lww.com/PAIN/B626. The standard CAJIS score is a physician-determined assessment.[31] We used a modified CAJIS (mCAJIS) score determined by assigning a numerical value to the following body areas, whether or not extra bone growth was present: neck, jaw, upper or lower back or chest, right shoulder, left shoulder, right elbow, left elbow, right wrist, left wrist, right hip, left hip, right knee, left knee, right ankle, or left ankle. Patient responses were assigned a score according to the following: "no" or "yes but movement is not affected" was assigned a score of 0, "yes and causes partial or limited movement" was assigned a score of 1, and "yes and causes total loss of mobility" was assigned a score of 2. The mCAJIS score was then calculated by summing the numerical scores. Only patients who respond to all 17 body parts were included in the mCAJIS score correlation.

2.2. Quantitative sensory testing study subjects

Adult patients with FOP seen at the UCSF Metabolic Bone Clinic or at a patient meeting were recruited to complete a pain history questionnaire and QST. Subjects were excluded from participation in this study if they had clinical signs of a FOP flare (characterized by new focal pain, swelling, injury, stiffness, or decreased range of motion), had known cognitive or neurological impairment that precluded completion of testing instruments or following instructions for QST, or were receiving any type of interventional study medication, such as palovarotene or imatinib. Healthy family members were recruited into our study as controls. Informed consent was obtained from the participant or legal guardian as appropriate. The Institutional Review Board at UCSF approved the study, which was funded by Department of Anesthesia and Perioperative Care, University of California, San Francisco.

2.3. Quantitative sensory testing

A modified QST protocol that has been previously validated[58] was used in our study. Using the Medoc TSAII NeuroSensory Analyzer (MEDOC, Israel) thermode with contact area of 9 cm^2 attached to the thenar eminence of the left hand, we measured cold detection threshold, warm detection threshold, and cold and heat pain thresholds. The baseline temperature was 32°C; the stimulus range was 0 to 50°C. To align QST data for age, gender, and test site, raw thermal data from each subject were transformed into Z-score using the equation Z-score = (Value$_{patient}$ − Mean$_{controls}$)/SD$_{controls}$ and published data obtained from healthy volunteers.[5,42,58] A negative Z-score represents a loss of function, and a positive Z-score represents a gain of function. Differences in the Z-scores of pain thresholds and detection thresholds between patients with FOP and controls were determined using Mann–Whitney *U* tests. A *P*-value $\leq$ 0.05 was considered statistically significant. Mechanical detection threshold and mechanical pain threshold (MPT) were measured with the up–down method, using von Frey filaments (North Coast) that exerted forces of pressure on bending between 0.026 g and 110 g and applied to the thenar eminence of the left hand. Quantitative sensory testing was conducted by the same investigator to limit operator variability.

2.4. Animals and surgery

Adult mice (4-12 week old) were used in all experiments. Wild-type C57BL/6 mice and MAFIA (CSF1R-EGFP-NGFR/FKBP1A/TNFRSF6) transgenic mice[8] (Stock #005070) were obtained from the Jackson Laboratory. For the spared nerve injury (SNI) model of neuropathic pain,[61] we ligated and transected the sural and superficial peroneal branches of the sciatic nerve under isoflurane anesthesia, leaving the tibial nerve intact. All animal experiments were approved by the Institutional Animal Care and Use Committee at UCSF and were conducted in accordance with the NIH Guide for the Care and Use of Laboratory animals.

2.5. Induced pluripotent stem cell culture and CRISPR genetic modification

Human iPSCs lines (non-FOP lines 1323 and WTc11 and FOP lines FOP1 and FOP3)[44] were maintained on SNL feeders, fed with mTeSR1 (Stem Cell Technologies, Vancouver, Canada), lifted enzymatically with Accutase (Stem Cell Technologies), and passaged, as previously described.[44] Cells were transitioned to Matrigel culture for 2 passages (to deplete feeder cells) before differentiation. ROCK inhibitor (Y-27632) was used to prevent apoptosis when cells were split, frozen, or thawed.[44] A CRISPR guide RNA was designed using the MIT CRISPR web tool (http://crispr.mit.edu) to introduce a

double-stranded break within 4 base pairs of the 617G > A point mutation in *ACVR1*. The final guide was selected based on the absence of predicted off target locations in known BMP pathway constituents. The crRNA (5′/AltR/rGrGrCrUrCrCrArGrArUrUrArCrArCrUrGrUrGrUrUrUrArGrArGrCrUrUrGrCrUr/AltR2/-3′) was complexed with fluorescently labeled tracer RNA (IDT, # 1075927) and packaged into the ribonucleoprotein complexes (IDT Alt-R Cas9 nuclease V3, #1081058, with RNAiMAX, #13778100) for transfection and then mixed with 50 ng of homology arm repair template to introduce the G > A mutation (5′TTCCTTTTCTGGTACAAAGAACAGTGGCTC**A**CCAGATTACACTGTTGGAGTGTGTCGGTA3′). Fifty microliter of this ribonucleoprotein complex in Opti-Mem was added to 0.1 mL of iPSC suspension (40,000 cells). After ~ 24 hours of incubation, transfection efficiency was estimated by microscopy for the tracer RNA. Sib selection was performed as previously described[47] using Matrigel or SNL feeder coated 96-well plates. At near confluence, DNA was harvested by scratching half of each well to release iPSCs into the media and then harvesting for DNA extraction. The remaining pool of cells were dissociated and cultured for the sib selection process. Digital droplet PCR (ddPCR) was used to detect the most positive wells to propagate in further sib selections. Primers for *ACVR1* (Forward = GGAGCTATATTGCTCAATCG, Reverse = CCGACACACTCCAACAGT) were combined with TaqMan probes specific for the ACVR1 617G > A (5'-/5HEX/TGG-CTC-ACC/ZEN/AGATT/3IABkFQ/-3', from IDT) or wild type (5'-/56FAM/AGT-GGC-TCG/ZEN/CCA-GAT/3IABkFQ/-3', from IDT), designed using Primer Express 3.0 (Applied Biosystems, Waltham, MA). After optimization, ddPCR was conducted using a QX100 or QX200 (BioRad, Hercules, CA) Droplet Generator, with an annealing temperature of 63.1°C. Samples were read using a QX100 Droplet Reader following the manufacturer's instructions. After 3 rounds of serial sib selections to enrich the mutant population, individual clones were isolated by low-density plating of 1000 cells onto a 10 cm plate coated with SNL feeders, as iPSCs carrying the $ACVR1^{R206H}$ mutation can be less stable and show higher propensity to differentiate spontaneously.[44] To aid in mutant enrichment, 100 nM of the BMP pathway inhibitor LDN-193189 (LDN) was added to daily culture.[34] Colonies were subsequently picked using a dissecting microscope and expanded on SNL feeder-coated 24-well or 96-well plates, with the assistance of cloning cylinders. Of the 120 colonies screened, 5 colonies were identified with high percentages of cells carrying the $ACVR1^{R206H}$ mutation. Only 1 clone ($WTc11^{R206H}$-3H) showed consistent high percentages of cells carrying the mutation and was thus selected for more detailed analysis. The parental WTc11 clone (WTc11-2F) was matched for similar passage numbers as a control. Clones 3H and 2F were thus used as an isogenic pair for experiments. Fingerprint analysis confirmed derivation from the WTc11 stock and showed no other major genetic perturbations; exome sequencing (UCSF Genomics Core) and subsequent variant identification using Annovar (annovar.openbioinformatics.org) identified the *ACVR1* 617 G > A mutation as the only major pathogenic variant difference between the 3H and 2F clones.

2.6. Western blotting

Parental WTc11 (2F) and $WTc11^{R206H}$ (3H) iPSC clones were plated at a density of approximately 50,000 cells per well in a 24-well Matrigel-coated plate. When they reached 70% to 80% confluency, the medium was replaced with serum-free medium (KO-DMEM, Gibco) for 1 hour followed by the addition of 50 ng/mL of Activin A (PeproTech, Cranbury, NJ) for 1 hour. The media was removed, and the cells were washed with 0.5 mL of cold DPBS. The cells were harvested on ice in 50 μL lysis buffer (RIPA, protease inhibitor, phosphatase inhibitor, sodium vanadate, and sodium fluoride) and stored at −80°C until purified. Protein was purified by serial centrifugation x 3 and quantified using a BCA standard assay (Thermo Fisher Scientific, Waltham, MA, #23225). Protein lysates of iSNs were obtained in the same fashion. Samples were denatured in SDS/BME at 95°C for 5 minutes; 12 to 15 μg of each iPSC sample and 5 μg of each iSN sample were loaded onto an SDS or PAGE gel (8%-16%), separated by protein electrophoresis, and transferred to a low-fluorescence PVFD membrane (Azure Biosystems, Dublin, CA). The membranes were incubated overnight with the primary antibody at a concentration of 1:1000 and probed the following day using a secondary HRP-conjugated antibody at 1:5000. Primary antibodies directed against pSMAD 1/5/9 (Cell Signaling Technology, D5B10, #13820S, anti-rabbit) and GAPDH (Cell Signaling Technology, Danvers, MA, anti-mouse, D4C6R) were used. Chemiluminescent signal was measured using an Azure Biosystems c300 imager (Azure Biosystems), and quantification was performed using Image J software. All samples were normalized to the expression of GAPDH.

2.7. Induced pluripotent stem cell differentiation into sensory neurons

Human sensory neuron differentiation was performed using a modified version of a published protocol.[12,13] In brief, iPSCs were seeded on a Matrigel-coated plate and maintained in mTeSR medium (Stem Cell Technology). Neural induction started once the cells reached 80% confluence by adding KSR medium consisting of Knockout DMEM and Knockout Serum Replacement (Gibco, Waltham, MA). 100nM LDN-193189 and 10μM SB-431054 (Tocris, Minneapolis, MN) were added from day 0 to 5 (DD0-DD5). N2 media consisting of Neurobasal media (Gibco) and 1X N2 Supplement (Gibco) were added starting at day 4 in concentration increments of 25% every other day, reaching 100% at day 10. Nociceptor induction started on day 2 by adding 3μM CHIR99021, 10μM SU5402, and 10μM DAPT (Tocris). Starting on day 11 (DD10), the cells were maintained in N2 media supplemented with 25ng/mL of human β-NGF, BDNF, and GDNF (PeproTech).

2.8. Electrophysiology

iPSCs were seeded on 15-mm tissue culture–treated plastic coverslips (Nunc Thermanox) coated with Matrigel in a well of a 12-well plate. 14 to 15 days postdifferentiation (DD14-15), coverslips were transferred from the culture media to a recording chamber constantly perfused with fresh recording medium containing 145 mM NaCl, 3 mM KCl, 3 mM $CaCl_2$, 10 mM HEPES, and 10 mM glucose at 32°C (pH 7.3-7.4 and osmolarity 290-300). Whole-cell patch-clamp recordings were performed using a phase-contrast inverted microscope (BX51W1, Olympus). The patch electrodes were constructed from borosilicate glass capillaries (Sutter Instruments, Novato, CA) with a resistance of 5 to 7 MΩ. The pipettes were tip filled with internal solution and then back filled with internal solution containing 125 mM potassium gluconate, 15 mM KCl, 10 mM HEPES, 4 mM $MgCl_2$, 4 mM Na_2ATP, 0.3 mM Na_3GTP, and 0.2 mM EGTA (pH 7.3-7.4 and osmolarity 290-300). Recordings were performed with an Axon Multiclamp 700B patch-clamp amplifier and 1440A Digitizer (Axon Instruments, San Jose, CA). Signals were filtered at 10kHz using amplifier circuitry, sampled at 100 kHz, and analyzed using Clampex 10 (Axon Instruments). Voltage-gated sodium and potassium currents were recorded on stepped voltages (−120 mV ~ +50 mV, 500 ms duration) stimulation under voltage-clamp mode in which the recorded cell was held at

−70 mV. The peak of voltage-gated sodium current was determined as the peak amplitude of fast inward current on membrane depolarization (peak amplitude of inward current within 0 ~ 10 ms during stepped voltage stimulation). The peak of voltage-gated potassium current was determined as the average amplitude of sustained currents (average amplitude of sustained currents between 400 and 500 ms during stepped voltage stimulation). The quality of recorded cells was analyzed by the formation of Giga-seal and intrinsic membrane characteristics measured immediately after rupture of the cell membrane. The recorded cells were filtered through the following criteria: First, the cell could form Giga seal with the recording pipette during establishment of whole-cell recordings; second, after rupture of the cell membrane, the leak current in the voltage-clamp mode was smaller than −100 pA; and third, the resting membrane potential of cells (recorded in current clamp I = 0 mode) was more negative than −30 mV and could be held at −60 mV under the current-clamp mode. The cells that did not meet the above criteria were excluded for statistical analysis.

2.9. Multielectrode array

Accutase (StemCell Technology)-dissociated neurons were seeded at a density of 5 to 10 x 10^4 cells per well to fully cover all 16 embedded electrodes in a 24-well CytoView MEA plate (Axion Biosystems, Atlanta, GA) precoated with 0.1% polyethleneimine (PEI) and 300 μg/mL of Matrigel. iSNs were then cultured for at least 2 weeks to from the functional networks before analysis. Real-time well-wide neuronal spontaneous firings with a spike detection criterion of >6 STDs were recorded with MaestroEdge (Axion Biosystems) for 3 to 5 minutes at 37°C. Data were analyzed with AXIS Navigator and AXIS Neural Metric Tool. Only the cells in a well with at least 7 active electrodes were used for analysis, and the firing rate based on active electrodes was presented as the weighted mean firing rate. In the experiments with compound treatment, after the baseline firings were recorded, iSNs were then stimulated with 1 μM capsaicin (TRPV1 agonist), 100 μM AITC (TRPA1 agonist), or 100 μM menthol (TRPM8 agonist) (Sigma Aldrich, St. Louis, MO). The evoked neuronal activity was immediately recorded. Recovery for at least 24 hours is required between each treatment. In the study with Activin A stimulation, iSNs were incubated with Activin A (50ng/mL, R&D) for 30 minutes. All iSNs were allowed to recover for at least 24 hours before the next treatment.

2.10. Immunohistochemistry

Human cells grown on 13-mm or 15-mm borosilicate coverslips pretreated with Matrigel were fixed in 4% paraformaldehyde for 15 minutes at room temperature and washed twice with PBS. The cells were incubated with primary antibodies for 24 hours at room temperature (RT). The cells were then washed with PBS and incubated with secondary antibodies at RT for 2 hours. The following antibodies were used for immunostaining: mouse anti-TuJ1 (1:100, R&D MAB1195), rabbit anti-Brn3a (1:500, Millipore #AB5945), rabbit anti-Peripherin (1:2000, Abcam, AB4666), guinea pig anti-TRPV1 (1:2000, gift from David Julius), rabbit anti-pSMAD1/5 (1:800, Cell Signaling #9516), and fluorophore-coupled secondary antibodies (1:1000, Alexa Fluor 488, 555, 594, 647, Thermo Fisher Scientific). Images were captured with a Carl Zeiss LSM 700 microscope and processed with Fiji/ImageJ (NIH).

For mouse DRG staining, mice were anesthetized with 2.5% Avertin and perfused transcardially with 1X PBS followed by 4% formaldehyde. Dissected DRG were first postfixed in the same fixative for 3 hours and stored overnight in 30% sucrose in PBS at 4°C before cryostat sectioning. The following primary antibodies were used for immunostaining: chicken anti-GFP (1:2000, Abcam #AB13970) and rabbit anti-ACVR1 (1:1000, Invitrogen #PA5-85263).

2.11. In situ hybridization

We used the RNAscope Fluorescent Multiplex Reagent Kit (Advanced Cell Diagnostics, Newark, CA) according to the manufacturer's instructions. In brief, iSNs grown on glass coverslips were first mounted on slides and then quickly frozen on dry ice. Freshly dissected mouse DRG were also frozen on dry ice before further cryostat sectioned at 12 μm and mounted on slides. The iSNs on coverslips or mounted sections were fixed in prechilled 10% neutral-buffered formalin for 15 minutes at 4°C. After a series of dehydration steps in gradient ethanol solutions, the sections were pretreated with Protease K for 30 minutes at room temperature and then incubated with RNA probe for 2 hours at 40°C in a HybEZ oven. Repeated washing and amplifier hybridizations were performed according to the manufacture's protocol. Finally, sections were costained with DAPI. The following probes were used: mouse *Acvr1* (#312411) and mouse *Atf3* (#426891) for DRG and human *TRPV1* (#415381) for iSNs.

2.12. Image quantification

To quantify the ISH message, we used ImageJ and analyzed signal intensity in a sensory neuron-rich region of the DRG (5-8 sections from the same ganglia; 3 mice per group). An individual blinded to the treatment groups performed the image analysis.

2.13. Gene expression

Total RNA was harvested from cells using TRIreagent (Sigma Aldrich) and chloroform (Sigma Aldrich), precipitated with isopropanol and ethanol, and resuspended in DNase/RNAse free water. cDNA was synthesized using the SuperScript III First Strand Synthesis system (Invitrogen, Waltham, MA). Quantitative RT-PCR was calculated using the $2^{-\Delta\Delta CT}$ method.[41] The following gene specific primers and fluorescent labeled TaqMan probes (Thermo-Fisher Scientific) were used: *ACVR1/Acvr1* (Hs00153836_m1 and Mm01331069_m1), *ALK3/BMPR1A* (Hs01034909_g1), *ID1* (Hs00357821_g1), *GAPDH* (Hs02758991_g1), or */β-actin* (Hs99999903_m1 or Mm02619580_g1) as the internal control for each sample.

2.14. Statistical analysis

Statistical analysis was performed using GraphPad Prism version 7.0 (GraphPad Software, San Diego, CA). Mann–Whitney *U* tests or Student *t* tests were used for single comparisons between 2 groups. Other data were analyzed using one-way or two-way analysis of variance (ANOVA). $^*P < 0.05$, $^{**}P < 0.01$, $^{***}P < 0.001$, and $^{****}P < 0.0001$, *NS*, nonsignificant.

3. Results

3.1. Neuropathic pain is common in a self-reported cohort of patients with fibrodysplasia ossificans progressiva

To identify if neuropathic pain is a major manifestation of FOP, we first queried the IFOPA FOP Connection Registry, an international survey-based patient database[43] (**Fig. 1**). As neuropathic pain is

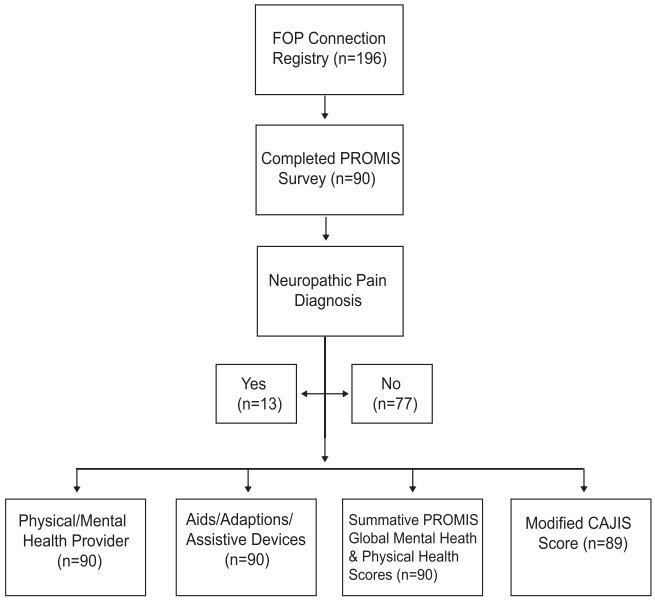

Figure 1. Flowchart of the IFOPA survey study design. IFOPA, International Fibrodysplasia Ossificans Progressiva Association.

generally rare in young children,[74] we limited our analysis to patients older than 15 years of age. Of the 196 patients with FOP spanning 42 countries who were asked to complete both PROMIS Global Health Survey and Aids/Adaptations/Assistive Devices Survey[11] from August 2017 to November 2018, 90 patients completed the survey. The demographics and clinical characteristics of our participants are outlined in **Table 1**. 14.4% of the patients self-reported neuropathic pain (**Table 1**). This incidence differs considerably from a prior large cohort data indicating a general population prevalence of neuropathic pain of 6.9% to 10%.[16,72]

Consistent with evidence that chronic pain is influenced by both physical and affective factors,[75] we found that patients with neuropathic pain had significantly more visits to medical providers for physical or mental health than those without neuropathic pain (**Table 2**). However, neither PROMIS Global Physical Health score nor PROMIS Global Mental Health score[23] differed between the 2 groups (**Table 2**). As the sensitivity of the PROMIS Global Mental Health score analysis can be confounded by the quality of life measure, which is generally not highly correlated with mental health,[23] we confirmed that a subanalysis performed after the removal of the quality of life measure did not change our conclusion (**Table 2**). Moreover, PROMIS Mental Health scores in the participating patients with neuropathic pain did not differ from those without neuropathic pain, arguing against a significant contribution of affective components to the severity of neuropathic pain symptoms in patients with FOP.

We also compared the functional impairment in patients with and without neuropathic pain. A modified Cumulative Analog Joint Involvement Score (mCAJIS) was used to assess the involvement of joint-specific diseases[31] based on patient-recorded joint involvement. Although the mCAJIS results did not statistically differ between the 2 groups, a significantly higher number of aids, assistive devices, and adaptations were used by patients with neuropathic pain (Tables 2 and S1). Therefore, we concluded that neuropathic pain is not only common in patients with FOP but is also associated with increased functional disability.

Table 1

Demographic and clinical characteristics of the International Fibrodysplasia Ossificans Progressiva Association (IFOPA) registry cohort queried in this study.

Total	Statistic	Total	With neuropathic pain	No neuropathic pain
Total	N (%)	90 (100%)	13 (14.4%)	77 (85.6%)
Gender	N (%)			
Male		27 (30.0%)	1 (7.7%)	26 (33.8%)
Female		63 (70.0%)	12 (92.3%)	51 (66.2%)
Current age (y)	Mean ± SD	35.0±12.38	34.5±13.07	35.1±12.35
	Median	31.5	29.0	32.0
	(Min, Max)	(19.0, 74.0)	(21.0, 60.0)	(19.0, 74.0)
Residing location (continent)	N (%)			
Africa		2 (2.2%)	0 (0%)	2 (2.6%)
Asia		5 (5.6%)	1 (7.7%)	4 (5.2%)
Europe		27 (30.0%)	1 (7.7)	26 (33.8%)
North America		36 (40.0%)	10 (76.9%)	26 (33.8%)
Oceania		6 (6.7%)	1 (7.7%)	5 (6.5%)
South America		14 (15.6%)	0 (0%)	14 (18.2%)
Type of FOP	N (%)			
Classic (R206H)		39 (43.3%)	5 (38.5%)	34 (44.2%)
Variant		6 (6.7%)	2 (15.4%)	4 (5.2%)
Unknown (no genetic testing)		44 (48.9%)	6 (46.2%)	38 (49.4%)
Missing		1 (1.1)	0 (0%)	1 (1.3%)
Age at diagnosis (y)	Mean ± SD	9.2±8.04	11 ± 12.11	8.9 ± 7.21
	Median	7.0	9.0	7.0
	(Min, Max)	(0.1, 48.0)	(1.2, 48.0)	(0.1, 37.0)
Age at first FOP symptom onset (y)	Mean ± SD	7.1±7.07	7.9 ± 12.27	7.0 ± 5.89
	Median	5.0	4.0	5.0
	(Min, Max)	(0.1, 45.0)	(0.1, 45.0)	(0.1, 26.0)

Table 2

Summary of the survey results based on patient-reported diagnosis of neuropathic pain at the time of enrollment into IFOPA FOP Registry.

Total	Statistics	Neuropathic pain (+)	Neuropathic pain (−)	*P*
# Times visited a doctor for physical health	N	13	77	
	Mean ± SD	6.6 ± 5.01	4.2 ± 5.18	*0.0255**
	Median	6.0	2.0	
	(Min, max)	(1.0, 16.0)	(0.0, 25.0)	
# Times visited a doctor for mental health	N	13	77	
	Mean ± SD	4.0 ± 8.15	2.0 ± 7.72	*0.022**
	Median	1.0	0.0	
	(Min, max)	(0, 30.0)	(0, 60.0)	
PROMIS Global Physical Health Score	N	13	77	
	Mean ± SD	2.8 ± 0.32	2.8 ± 0.73	*0.9537*
	Median	2.8	2.8	
	(Min, max)	(2.0, 3.3)	(1.3, 5.0)	
PROMIS Global Mental Health Score	N	13	77	
	Mean ± SD	2.9 ± 0.85	3.2 ± 0.89	*0.1758*
	Median	3.0	3.3	
	(Min, max)	(1.3, 4.3)	(1.0, 4.8)	
PROMIS Global Mental Health Score without Quality of Life Score	N	13	77	
	Mean ± SD	2.8 ± 0.92	3.3 ± 0.90	*0.0997*
	Median	3.0	3.3	
	(Min, max)	(1.3, 4.3)	(1.0, 4.7)	
Quality of Life Score	N	13	77	
	Mean ± SD	2.9 ± 0.95	3.0 ± 1.22	
	Median	3.0	3.0	
	(Min, max)	(1.0, 4.0)	(1.0, 5.0)	*0.8633*
Total PROMIS Global Health Score	N	13	77	
	Mean ± SD	30.5 ± 6.44	32.3 ± 8.42	*0.4903*
	Median	31.0	31.0	
	(Min, max)	(15.0, 38.0)	(13.0, 51.0)	
Total Modified CAJIS Score (mCAJIS)†	N	12	67	
	Mean ± SD	18.8 ± 9.77	15.3 ± 7.80	*0.2620*
	Median	17.5	15.0	
	(Min, max)	(5.0, 33.0)	(0.0, 34.0)	
Aids, assistive devices, and adaptations	N	13	77	
	Mean ± SD	22.5 ± 14.52	14.7 ± 10.04	*0.0426**
	Median	25.0	13.0	
	(Min, max)	(1.0, 51.0)	(0.0, 49.0)	

Statistical significance was determined by the Wilcoxon rank-sum test comparing "with" and without" neuropathic pain.

* $P < 0.05$.

† Calculated based on patient-reported joint involvement.

3.2. Patients with fibrodysplasia ossificans progressiva have mechanical and heat pain hypersensitivity

Inequity in global awareness of neuropathic pain[36] and poor patient education about the definition and presentation of neuropathic pain in many musculoskeletal pain conditions[39] have raised concerns that the true global prevalence of neuropathic pain in patients with FOP could be underestimated in the IFOPA registry surveys. Notably, in one cohort,[35] 23 to 31% of patients with FOP reported some form of somatosensory change (including but not limited to neuropathic pain) at baseline. As clinical diagnosis of neuropathic pain requires accurate medical characterization and sensory examination,[20] we identified a cohort of patients with FOP for more detailed in-person study in which investigators could uniformly define and assess for neuropathic pain. From August 2017 through May 2018, we enrolled 9 FOP adult subjects without ongoing flares (FOP, mean age of 30.7 years) and 10 healthy control family members (Ctrl-f, mean age of 48.2 years) from the UCSF Metabolic Bone Clinic for QST testing (**Fig. 2A and B**). All FOP adults were confirmed to carry a classical *ACVR1*^{R206H} mutation. Importantly, because the biological heritability in chronic pain is estimated to range from 29% to 50%,[25] direct comparison with family members would limit the contributing confounders to the patient's pain sensitivity.

We first characterized the baseline pain of our study cohort by having participants complete a questionnaire (Table S2, http://links.lww.com/PAIN/B626). In our cohort, 89% of study patients with FOP experienced pain in the past 6 months; only 20% of family members reported some form of pain during the same period. Notably, persistent pain occurred in 66% of patients with FOP but not by any of their family members. In patients with FOP, the pain was mainly located in the lower back (55%) and lower extremity (88%). Only 20% of family members experienced either back or lower extremity pain. In patients with FOP, 66% had a history of opioid exposure and 88% had used a traditional neuropathic pain medication (eg, gabapentin). By comparison, only 20% of family members had a history of opioid use and 30% had used neuropathic pain medications. Importantly, abnormal sensation (ie, tingling, sensitive to temperature or pressure, etc.)

was present in up to 55% of patients with FOP. None of their family members reported similar sensory symptoms. Taken together, more than half of the enrolled patients carrying a classical ACVR1^{R206H} mutation had chronic pain with symptoms of a neuropathic pain phenotype.

To define the altered sensory function of patients with FOP, we conducted QST, the clinical "gold standard" for assessing clinical function of small diameter, A-σ and C primary sensory neurons. These afferent fibers transmit noxious thermal and mechanical inputs,[21] and using QST, we can determine an individual's thresholds for both detection and pain. After adjustment for both sex and age,[58] we converted the thresholds to Z-scores of patients with FOP and healthy family members (Ctrl-f). Neither cold nor warm detection thresholds (cold detection threshold and warm detection threshold, respectively) differed between the 2 groups (**Fig. 2C–F**). Although patients with FOP had higher cold pain threshold (cold pain sensitivity) than their family members (**Fig. 2G**), the adjusted Z-scores did not differ (**Fig. 2H**). Importantly, adult patients with FOP had significantly lower heat pain threshold (reflected by higher Z-scores) compared with their healthy family members (**Fig. 2I–J**).

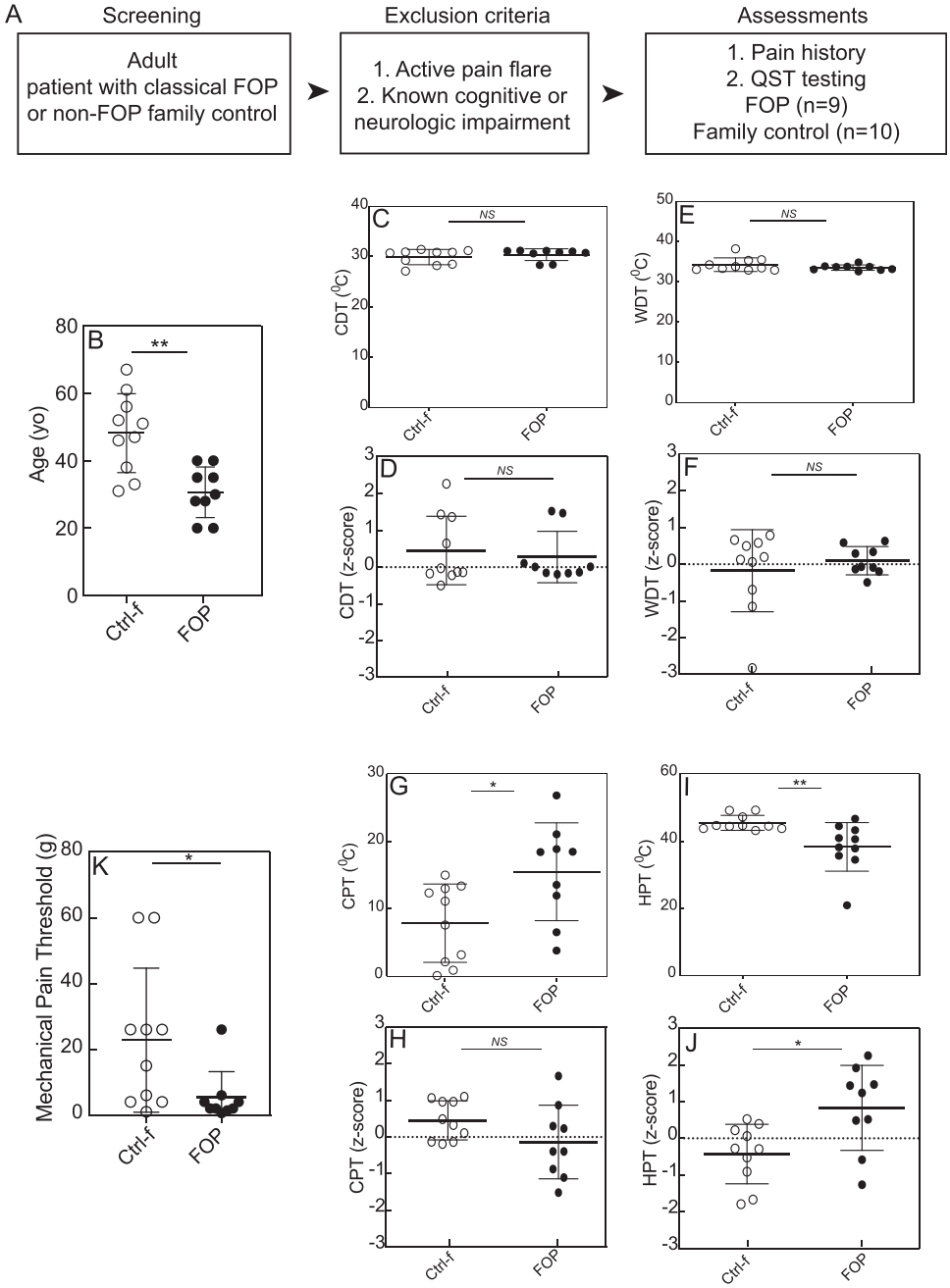

Figure 2. QST shows abnormal mechanical and heat pain hypersensitivity in adult patients with FOP. (A) Flowchart depicting patient enrollment in QST. (B) Age comparison in adult patients with FOP (FOP) and healthy family members (Ctrl-f). (C–J) Comparison of thermal thresholds between adult patients with FOP (FOP) and healthy control family members (Ctrl-f). The cold detection threshold (CDT, C), warm detection threshold (WDT, E), cold pain threshold (CPT, G), and heat pain threshold (HPT, I) were converted to Z-scores after adjustment of sex and age (D, F, H, and J, respectively). (K) Assessment of the average mechanical pain threshold (MPT) using QST assessing amount of force tolerated using von Frey filaments in the FOP group and healthy family members. Data presented as mean ± SD. Mann–Whitney *U* test in B-G. **P* < 0.05; ***P* < 0.01; *NS*, nonsignificant compared with control. QST, quantitative sensory testing.

Although, MPT is reportedly higher in older people,[58] we found that adult patients with FOP had a significantly lower MPT compared with their healthy family members (**Fig. 2K**). However, because there is no reliable von Frey comparator database from healthy volunteers, which would make it possible to convert the raw data of our mechanical pain threshold into Z-scores for comparison, we studied an additional 9 nonrelated age and sex-matched healthy volunteers (Ctrl) (Fig. S1A, http://links.lww.com/PAIN/B626). Again, we found that the average mechanical pain threshold was significantly lower in the FOP group than in the nonrelated healthy volunteer group (Fig. S1B, http://links.lww.com/PAIN/B626). Together, we conclude that adult patients with FOP have significant nociceptive hypersensitivity to both heat and mechanical stimuli at baseline (ie, in the absence of a FOP inflammatory flare-up).

3.3. Peripheral nerve injury induces Acvr1 expression in the mouse dorsal root ganglia

Our finding that adult patients with FOP have nociceptive hypersensitivity led to the hypothesis that constitutive activation of ACVR1 by the R206H mutation in FOP contributes to the neuropathic pain phenotype. To address this hypothesis, we next examined whether ACVR1 was expressed in sensory neurons of the DRG. Using the SNI mouse model of neuropathic pain, which induces hypersensitivity of the hind limbs,[60] within 24 hours after SNI (POD1), we observed a 2-fold upregulation of *Acvr1* gene expression in the ipsilateral L4/L5 DRG, compared with the contralateral uninjured side (**Fig. 3A**). Importantly, by both immunostaining (**Fig. 3B and C**) and in situ hybridization (ISH) (**Fig. 3D–F**), we found that ACVR1 was exclusively expressed in DRG sensory neurons, not in surrounding non-neuronal cells. Furthermore, at POD7, we recorded a 1.5-fold induction of *Acvr1* that was limited to axotomized (*Atf3*$^+$) neurons. The expression in uninjured (*Atf3*$^-$) sensory neurons did not change. (**Fig. 3G**). Together, neuronal ACVR1 might contribute to neuropathic pain in normal individuals as well.

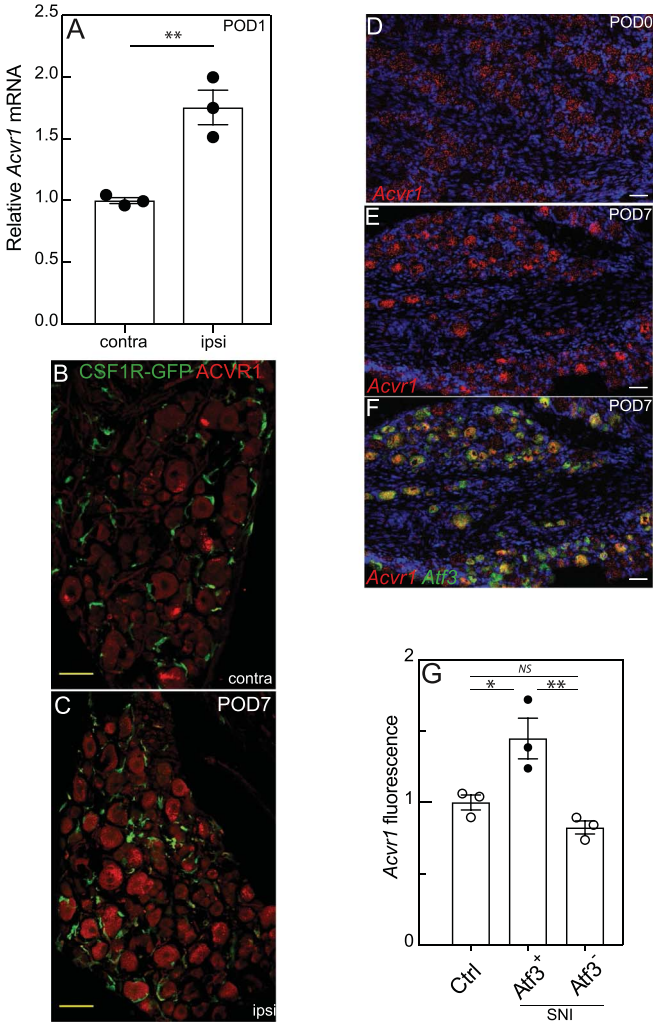

Figure 3. ACVR1 is selectively induced in axotomized mouse DRG neurons. (A) qRT-PCR of *Acvr1* expression in ipsilateral and contralateral L4/5 DRG 1 day after spared nerve injury (SNI, POD1) (n = 3 mice per group). (B-C) 7 days after SNI (POD7), immunoreactive ACVR1 (red) and CSF1R-GFP (green) in the DRG of MAFIA mice in which green fluorescent protein (GFP) under the control of the promoter of CSF1 receptor (CSF1R) is specifically expressed in macrophages. (D–G) In situ hybridization (ISH) analysis of *Acvr1* expression (red) in the DRG of mice before (POD0, D) and after nerve injury (POD7, E, F). *Atf3* labels axotomized sensory neurons (green, F), and nuclei were stained with DAPI. Data presented as mean ± SEM. Student *t* test in A, and one-way ANOVA with Tukey correction in G. *$P < 0.05$; **$P < 0.01$; *NS*, nonsignificant compared with control. Scale bar: 15μm in B-C, 50μm in (D–F). DRG, dorsal root ganglia.

3.4. Generation of nociceptive sensory neurons from patient-derived fibrodysplasia ossificans progressiva–induced pluripotent stem cell

We next asked how abnormal ACVR1 signaling might affect human sensory neuron function. Using a modified differentiation protocol[12,13,44,66] (Fig. S2A, http://links.lww.com/PAIN/B626), we generated nociceptor-like iSNs from patient-derived human iPSCs (FOP1 and FOP3) carrying the classical ACVR1^{R206H} mutation.[44] Two non-FOP iPSC clones (WTc11 and 1323) from healthy donors were used as a control group (Ctrl). At 2 weeks postdifferentiation, characteristics of sensory neurons were illustrated by coimmunostaining for neuronal marker TUJ1 and the sensory neuron marker BRN3a (Fig. S2B-D, http://links.lww.com/PAIN/B626).

Next, we examined BMP signaling in the iSNs. Expression of the key members of BMP signaling did not differ significantly between FOP and Ctrl iSNs (Fig. S2E-I), and there was no significant change in pSMAD1/5 expression when Ctrl iSNs were stimulated by Activin A (Fig. S2J-K, http://links.lww.com/PAIN/B626). By contrast, consistent with a previous report,[22] Activin A (AA) remarkably increased nuclear SMAD1/5 phosphorylation (pSMAD1/5) in FOP iSNs (Fig. S2L-M, http://links.lww.com/PAIN/B626).

To assess the electrophysiological characteristics of the iSNs, we performed whole-cell patch-clamp recording of iSNs and recorded action potentials (APs) at 2 weeks postdifferentiation (**Fig. 4A–C**). Notably, compared with control iSNs derived from 1323 clone, 1 of 2 derived FOP iSN lines (FOP3) had significantly more action potential numbers during maximal firing induced by current injection, although the FOP1 line showed a trend towards increased AP numbers (**Fig. 4D**). Importantly, the peak amplitudes of both voltage-gated Na^+ (**Fig. 4E**) and K^+ currents (**Fig. 4F**) were significantly increased in both FOP clones compared with the control. **Figure 4G** also shows that intrinsic cell membrane characteristics, including resting membrane potential (Vm), resistance (Rm), and capacitance (Cm) of sensory neurons, derived from all clones did not differ, which suggests similar neuronal subtypes were derived from all 3 cell lines. Specifically, there was no significant difference in membrane capacitance between the 3 groups of neurons when measured by whole-cell

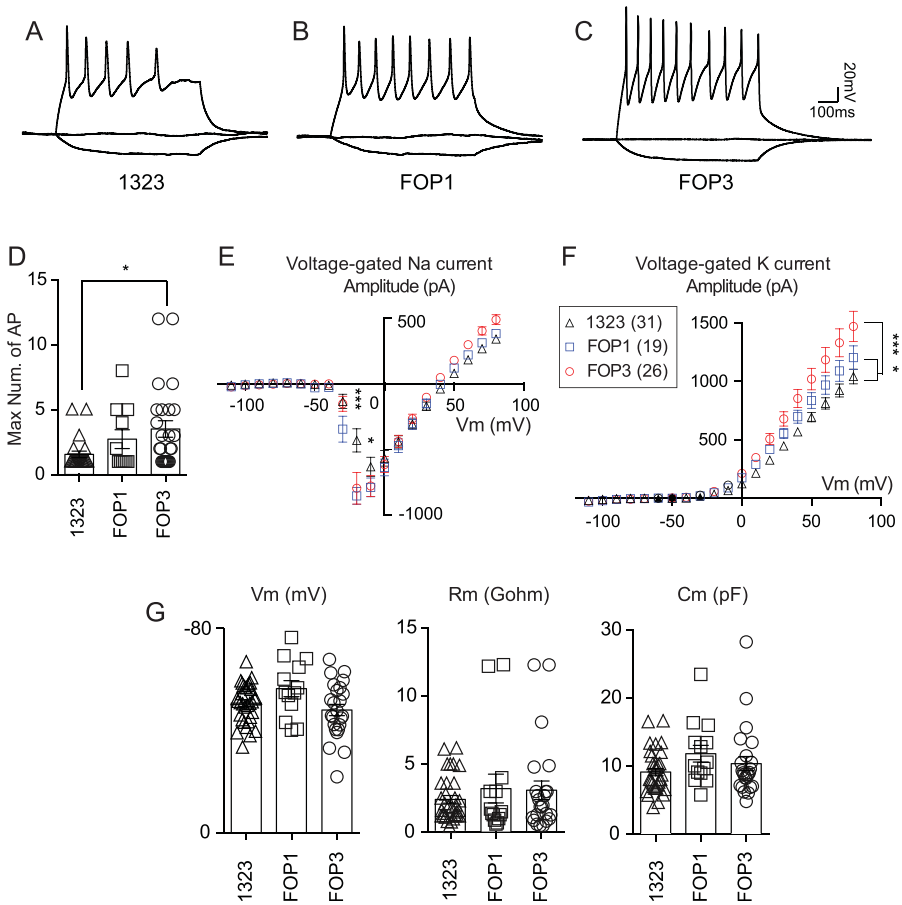

Figure 4. Whole-cell electrophysiological characterization reveals increased excitability in FOP iPSC–derived sensory neurons. (A–C) Representative AP firing pattern traces evoked in iSNs on near-threshold current injections. Scale bars represent 20 mV and 100 ms. (D) Statistical analysis of maximal number of AP firings on current injections. (E and F) I-V curve of Na^+ (E) and K^+ (F) currents measured under stepped voltages in the voltage-clamp mode (500ms duration, from −100 to +100 mV). Both the peak voltage-gated Na^+ and K^+ channel currents increased significantly in FOP iSNs compared with control (1323) iSN. (G) Resting-membrane potential (Vm), membrane resistance (Rm), and membrane capacitance (Cm) were unchanged in control and FOP iSNs. iSNs at 2 weeks postdifferentiation were used. Data represented as mean ± S.E.M. One-way ANOVA with a post hoc Bonferroni test in D-G. $^*P < 0.05$; $^{***}P < 0.001$; FOP, fibrodysplasia ossificans progressiva; iPSCs, induced pluripotent stem cells; NS, nonsignificant.

recordings and analyzed by one-way ANOVA (Ctrl: 8.98 ± 0.55 pF, n = 33; FOP1: 11.84 ± 1.22 pF, n = 14; FOP3: 10.27 ± 1.04 pF, n = 24. $P = 0.099$). Taken together, our results show that functional iSNs generated from both control (1323) and FOP iPSC clones had comparable intrinsic membrane characteristics. FOP iSNs carrying an $ACVR1^{RH206}$ mutation showed increased Na^+ and K^+ currents and were prone to fire repetitive action potentials.

It is possible that the increased APs in the $ACVR1^{R206H}$ iSNs resulted from clonal or inter-individual variability. To address this, we used CRISPR editing on the non-FOP WTc11 iPSC line to generate an isogenic clone ($WTc11^{R206H}$). We confirmed that this clone carried the expected $ACVR1^{R206H}$ mutation (Fig. S3A, http://links.lww.com/PAIN/B626) and found that it showed dramatically increased pSMAD1/5 phosphorylation in response to AA stimulation (Fig. S3B). At 2 to 3 weeks postdifferentiation, $WTc11^{R206H}$ iPSCs differentiated into $BRN3a^+$ $TUJ1^+$ iSNs (Fig. S3C, http://links.lww.com/PAIN/B626), in which intracellular pSMAD1/5 was induced by Activin A (Fig. S3D-E, http://links.lww.com/PAIN/B626).

Taken together, our findings demonstrate that functional iSNs can be generated with equivalent maturation from both control and $ACVR1^{R206H}$ iPSCs.

3.5. $ACVR1^{R206H}$ is both necessary and sufficient for hyperexcitability of iSNs in vitro

To provide more direct evidence that these iSNs can be used to model the hypersensitivity of patients with FOP, we maintained the iSNs in culture for more than 6 weeks to allow further maturation into functional nociceptive neurons.

In contrast to mice in which only 30% of DRG sensory neurons express TRPV1,[55,62] most human DRG neurons (>70%) express both *TRPV1* mRNA[62] and TRPV1 protein.[63] Moreover, the transcriptomes of human DRG further define *TRPV1* as a marker of most human nociceptor neurons.[68] At 6 to 8 weeks postdifferentiation, iSNs of all 4 lines expressed both peripherin (PRPH), a marker of small diameter sensory neurons, and human nociceptor marker TRPV1 (**Fig. 5A–D**). Furthermore, almost all $TUJ1^+DAPI^+$ iSNs were $TRPV1^+$ (**Fig. 5E**), depicting phenotypical resemblance with primary human nociceptors. Importantly, to address antibody specificity against human TRPV1, we subsequently used ISH and confirmed the expression of *TRPV1* in all iSNs examined (**Fig. 5F**). Next, we determined whether constitutive ACVR1 signaling remains functional during the differentiation. Here, we treated both WTc11 and $WTc11^{R206H}$ iSNs with 50 ng/mL of AA and then assessed pSMAD1/5 activity by

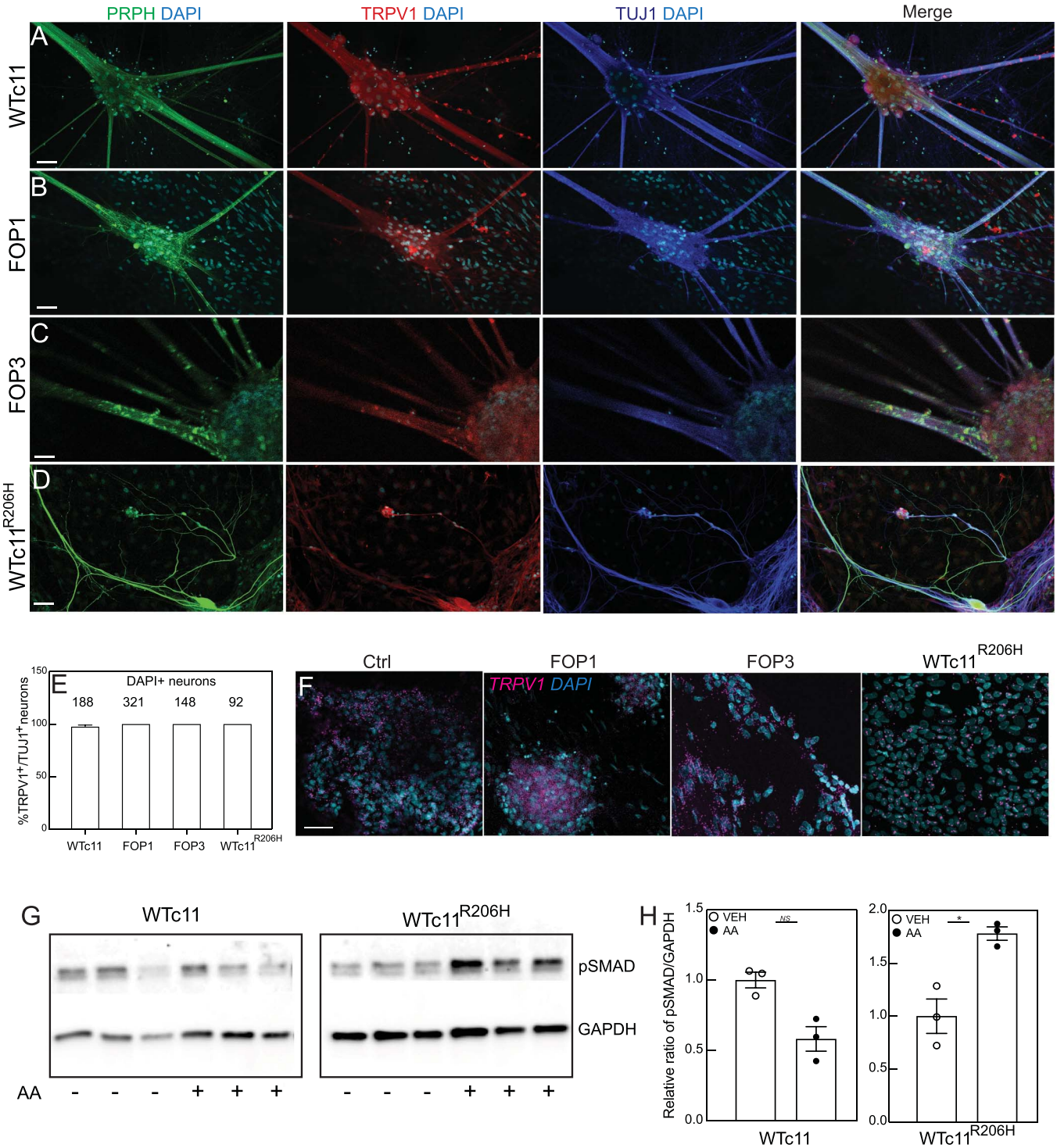

Figure 5. Generation of nociceptive iSNs from patient-derived iPSCs assessed 6 weeks postdifferentiation. (A–D) Representative images of iSNs coexpressing nociceptor marker Peripherin (PRPH, green), TRPV1 (red), and neuronal marker TUJ1 (blue). (E) Quantitation of $TRPV1^{+}/TUJ1^{+}DAPI^{+}$ iSNs. n = 3 to 4 independent experiments; 92 to 188 $DAPI^{+}$ neurons per clone were analyzed. (F) In situ hybridization (ISH) analysis of *TRPV1* expression (magenta) in iSNs. Nuclei were stained with DAPI. Scale bar: 50 μm in A-D and F. (G and H) Protein levels of pSMAD1/5 in iSNs of WTc11 and $WTc11^{R206H}$ treated with either Activin A (AA) or vehicle (VEH) for 60 minutes, as determined by Western blot (G) and densitometric analysis (H). GAPDH was used as a loading control. n = 3 experiments. Data presented as mean ± S.E.M. Student *t* test in H. $^{*}P < 0.05$; *NS*, nonsignificant compared with control.

Western blot (**Fig. 5G**). Quantitative densitometric analysis confirmed AA-induced pSMAD activity in $WTc11^{R206H}$ iSNs (**Fig. 5H**), By contrast, there was no increase in the pSMAD activity in WTc11 iSNs after treatment with AA.

In further functional analyses, we measured neuronal excitability by recording spontaneous extracellular field potentials generated by APs in live neurons plated onto a multielectrode array (MEA) (Fig. S4A-B).[65] **Figure 6A–C** illustrate robust persistent spontaneous neuronal firings from both non-FOP WTc11 and FOP iSNs; however, in both FOP lines, the neuronal firing rate was significantly higher than in WTc11 neurons (**Fig. 6A–C**). Notably, the spontaneous firing rate of FOP3 iSNs was

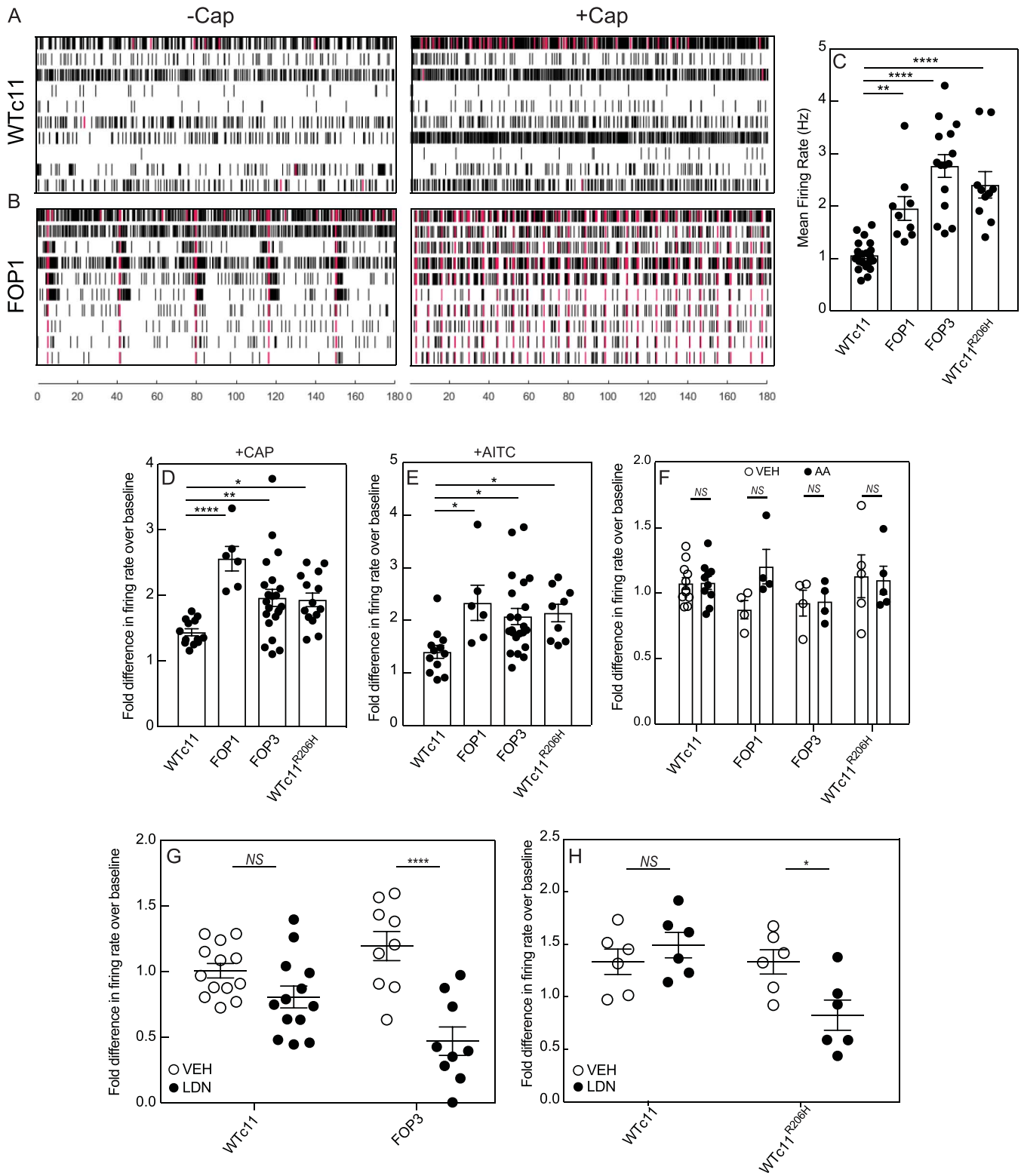

Figure 6. Extracellular electrophysiological characterization of iPSC-derived nociceptive sensory neurons by MEA. (A and B) Representative raster plots of firing spikes in response to capsaicin stimulation in control (WTc11) (A) and FOP1 iSNs (B). Burst firings (≥ 5 spikes per second) were highlighted in red. (C) Comparison of the mean firing rate at baseline (n ≥ 9 wells per group). (D–F) Effect of stimulation of capsaicin (1 μM, D), AITC (100 μM, E), or Activin A (50 ng/mL, F) on the neuronal firing rate (n ≥ 6 per group). (G–H) Effect of ACVR1 inhibitor LDN-193189 (LDN) on the neuronal firing rate. Neuronal activity was recorded before and after the cells were treated with either LDN-193189 (200nM) or VEH for 48 hours (n ≥ 9 per group). iSNs 6 to 10 weeks postdifferentiation were used for all MEA. Data represented as mean ± SEM. One-way ANOVA with a Dunnett test in C-E. Two-way ANOVA with a Sidak correction in F. Two-way ANOVA with a Tukey correction in G-H. *$P < 0.05$; **$P < 0.01$; ****$P < 0.0001$; NS, nonsignificant.

greatest among all 3 lines of iSNs (**Fig. 6C**), corroborating the whole-cell patch-clamp results (**Fig. 4D**). Furthermore, a low-dose of KCl (400μM) induced significantly greater neuronal activity in FOP3 iSNs compared with control iSNs (Fig. S4C, http://links.lww.com/PAIN/B626).

To assess the extent to which the variable differentiation environment rather than the genotype contributes to the experimental results, we compared control iSNs (WTc11) derived from 4 independent differentiations but found no significant variations in the neuronal firing rate (Fig. S4D). We conclude that a comparable degree of neuronal differentiation and maturation was consistently achieved. It is also possible that the increased firing rate recorded using MEA resulted from more neurons surviving after the initial plating. To address the question, we also dissociated iSNs after 3 weeks of culture in a 24-well MEA plate and confirmed that the number of viable cells did not differ among the WTc11, FOP1, and FOP3 groups (Fig. S4E). Most importantly, as WTc11^{R206H} iSNs exhibited hyperexcitability compared with the isogenic parental WTc11 iSNs (**Fig. 6C**), we concluded that ACVR1^{R206H} is sufficient for the enhanced neuronal excitability and that this is independent of clonal or interindividual variability.

Using MEA, we also examined neuronal responses to noxious stimuli and confirmed that the enhanced iSN activity can be induced by both the TRPV1 agonist, capsaicin (Cap) (**Figs. 6A, B and D**; Fig. S4F, http://links.lww.com/PAIN/B626), and the TRPA1 agonist, AITC (**Fig. 6E**). Interestingly, we found that these nociceptive sensory neurons did not respond to the TRPM8 agonist, menthol (Menthol^{-}) (Fig. S4G). Although it is possible that menthol-induced APs are below the MEA detection threshold, a recent report concluded that human Menthol^{+}Cap^{-}AITC^{-} iSNs constitute a mechanosensitive population.[50]

To further study the TRP channel properties of these iSNs, next we stimulated all 4 types of iSNs, including WTc11^{R206H} iSNs with 1 μM capsaicin or AITC (100 μM), and compared the magnitude of evoked neuronal response to baseline activity (**Fig. 6A, B and D**). We found that all ACVR1^{RH206} iSNs tested were significantly more responsive to capsaicin stimulation and to AITC than were the controls (**Fig. 6D and E**).

As Activin A can bind to the ACVR1^{R206H} receptor to induce abnormal cellular activity mimicking BMPs in many cell types[22] including iSNs, we examined if Activin A could potentiate the neuronal activity as described in rodents,[81] The firing rate of iSNs after Activin A or vehicle (VEH) treatment was compared with baseline without treatment (**Fig. 6F**). To our surprise, Activin A treatment did not further enhance the neuronal activity in all lines of iSNs we examined, suggesting that an intrinsic mechanism is involved.

We next asked if constitutively active ACVR1^{R206H} signaling was necessary for the neuronal hyperexcitability of the iSNs. In these studies, we examined the effect of LDN-193189 (LDN), a small molecule inhibitor of both ACVR1 and BMPR1A/ALK3.[49,79] LDN-193189 blocks signaling through the constitutively active ACVR1^{R206H} and reduces pSMAD1/5 in vitro and in vivo.[79] Here, we treated WTc11 and FOP3 iSNs with LDN-193189 or VEH for 48 hours, and using MEA, we compared neuronal activity (**Fig. 6G**). Control iSNs showed no significant change in the firing rate between the LDN-treated and VEH-treated groups. By contrast, LDN-treated FOP3 iSNs had significantly less spontaneous firing compared with the VEH-treated FOP group. Similarly, LDN treatment resulted in a significant reduction in firing rate of WTc11^{R206H} iSNs but not WTc11 isogenic control iSNs (**Fig. 6H**).

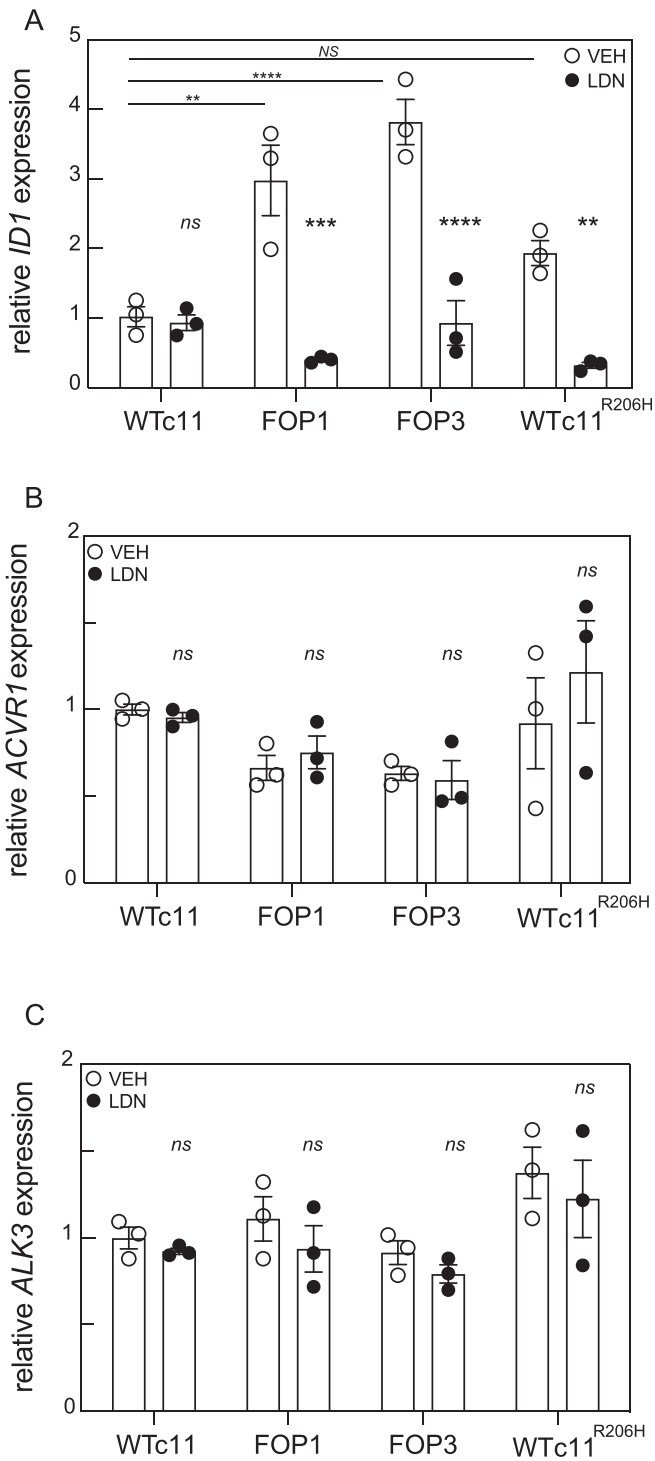

Figure 7. Quantitative RT-PCR analysis of BMP pathway in iSNs treated with LDN-193189. (A–C) mRNA expression of *ID1* (A), *ACVR1* (B), and *ALK3* (C) in iSNs treated with either LDN-193189 (200nM) or VEH for 48 hours (n = 3 experiments per group). iSNs 8 to 10 weeks postdifferentiation were used. Data represented as mean ± SEM. Two-way ANOVA with a Tukey correction. $^{**}P < 0.01$; $^{***}P < 0.001$; $^{****}P < 0.0001$; NS, nonsignificant.

Finally, to confirm that LDN-193189 indeed effectively inhibited ACVR1 signaling in the ACVR1^{R206H} iSNs, we used qRT-PCR and found that in all ACVR1^{R206H} iSNs examined, 2-day LDN treatment significantly inhibited the expression of *ID1,* a target gene downstream of ACVR1 (**Fig. 7A**). Notably, baseline *ID1* expression was higher in ACVR1^{R206H} iSNs than in WTc11, which

suggests that aberrant ACVR1 signaling remained active through differentiation. By contrast, expression of *ACVR1* or *ALK3* was not affected by LDN blockade (**Fig. 7B and C**), which highlights the selectivity of the LDN treatment.

Taken together, we concluded that ACVR1^{RH206} is both a necessary and sufficient contributor to hyperexcitability of iSNs in vitro.

4. Discussion

The BMP pathway, a key regulator of bone formation, is increasingly recognized to have important roles in multiple neurological processes.[17,29,30,40,70,82] However, the mechanisms through which ACVR1 variants contribute to neuronal dysfunction are unclear. We now demonstrate that adult patients with FOP, who have a classic activating mutation in the Type I receptor ACVR1 of the BMP pathway (ACVR1^{R206H}), have increased mechanical and heat pain hypersensitivity documented by QST. Of particular interest is our cellular finding that ACVR1^{R206H} is both necessary and sufficient for the hyperexcitability of iPSC-derived iSNs using both intracellular and extracellular recordings. Notably, ACVR1^{R206H} iSNs are more responsive to capsaicin or AITC stimulation. As *Trpv1*-mediated heat pain hypersensitivity is well investigated,[2] *Trpa1 is* arguably required for neuronal excitation and subsequent mechanical hypersensitivity.[3,67] Decreased responses to noxious mechanical force have been reported in *Trpa1*$^{-/-}$ mice.[37,38] As hyperexcitability of sensory neurons is considered a major contributor to neuropathic pain,[4] we suggest that ACVR1^{R206H} directly contributes to mechanical and heat pain hypersensitivity in patients with FOP. Moreover, in a mouse model of neuropathic pain, ACVR1 was selectively induced in axotomized DRG neurons, further supporting the functional relevance of ACVR1 in pain processing. Our findings may help explain the difficult-to-control baseline chronic pain commonly present in the patients with FOP. Although FOP is rare, its underlying pain mechanism may be shared by other chronic pain conditions in humans.

The ACVR1 receptor is required for several ligands of BMP signaling to trigger the downstream molecular and cellular responses.[22,24,56] In contrast to animal studies which reveal that Activin A sensitizes DRG neurons in neuropathic pain,[77,81] we found that Activin A does not have a significant contribution to the neuronal activity of iSNs in vitro. Inhibiting ACVR1 signaling in ACVR1^{R206H} iSNs substantially reduced the neuronal firing rate. Taken together, we conclude that ACVR1^{R206H} is sufficient and necessary to induce hyperexcitability of iSNs.

However, how exactly ACVR1 influences nociceptive processing in humans remains to be elucidated. It is conceivable that repetitive tissue injuries during HO flares or increased local BMP pathway activity may further sensitize the sensory neurons which are already hyperexcitable as baseline in patients with FOP; thus, the likelihood to develop neuropathic pain syndrome in adulthood could be remarkably increased. In addition, it was reported that *Acvr1* downstream target *Smad1* promoted injury-induced axonal regeneration,[14,51,57,59] which is closely associated with neuronal hyperexcitability and neuropathic pain development.[57]

Some limitations in our study should be noted. First, we were able to assess only a small number of patients with FOP using QST testing, because of the rarity of this disease and difficulty brings subjects onsite. The significant functional impairment of this population further limits their ability to travel or participate in studies. Notably, our cohort of sequentially enrolled QST participants showed a much higher frequency of clinically defined neuropathic pain, in contrast to the IFOPA registry survey data based on patients' self-reporting. Thus, the true incidence of neuropathic pain in patients with FOP is likely underreported on the IFOPA surveys. Second, although our study demonstrates that there is a significant incidence of sensory dysfunction in patients with FOP, even in the absence of a clinical HO flare, not all adult patients with FOP in our study showed clinically evident sensory dysfunction. It remains unclear if the ACVR1 gene environment is affected by epigenetic modification which has been previously implicated in the susceptibility to develop chronic pain.[15] Finally, although both whole-cell patch-clamp recording and MEA showed hyperexcitability of ACVR1^{R206H} iSNs, a hallmark of neuropathic pain,[71] neuroinflammation[27] may further contribute to the thermal and mechanical hypersensitivity observed in the patients with FOP.

As we previously reported, a reciprocal cellular interaction between macrophages and sensory neurons in the DRG contributes to the persistent neuropathic pain phenotype.[80] Recently, our group also showed that the primary monocytes or macrophages isolated from the patients with FOP are predominantly proinflammatory and induced by aberrant ACVR1 signaling.[1] Proinflammatory mediators released from macrophages can directly or indirectly sensitize sensory neurons and induce pain hypersensitivity.[2,9,27,32] This may involve macrophage production of Activin A.[45] Thus, it will be important to determine how immune cells contribute to the sensitization of sensory neurons in the patients with FOP.

In conclusion, our study shows that neuropathic pain with mechanical and heat pain hypersensitivity in the absence of ongoing inflammation is a major clinical component in FOP manifestations, and it is likely associated with underlying increased excitability of nociceptive sensory neurons and increased response to noxious stimuli secondary to ACVR1 dysfunction. Whether other conditions affecting the BMP/ACVR1 pathway have similar nociceptive phenotypes remains to be determined. Regardless, our results suggest that strategies for modulating ACVR1 signaling hold promise in the management of the chronic pain experienced by patients with FOP.

Conflict of interest statement

E.C. Hsiao serves in a volunteer capacity on the registry advisory board of the International Fibrodysplasia Ossificans Progressiva Association, the International Clinical Council on FOP, and on the Fibrous Dysplasia Foundation Medical Advisory Board. E.C. Hsiao, T. Chan, K. Bigay, and J. Ho receive clinical trials research support from Clementia Pharmaceuticals Inc, an Ipsen company, through their institution. E.C. Hsiao also received prior clinical trials research support from Regeneron Pharmaceuticals and Neurocrine Biosciences, Inc. These pose no conflicts for this study. The remaining authors have no conflicts of interest to declare.

Acknowledgements

The authors are grateful to all the FOP families participating in our studies. The authors also thank the Stem Cell Core at Gladstone Institutes for its technical support for MEA recording and a financial contribution from the Roddenberry Foundation for the MaestroEdge purchased by the Stem Cell Core.
Funding: The study was supported by a Clinical Seed Award from the UCSF Department of Anesthesia and Perioperative Care (X.Y.), Accelerating Cures and Treatments (ACT) grant from International FOP Association (X.Y.), UCSF New Frontiers Research (NFR) Award (X.Y. and E.C.H.), Howard Hughes Medical Institute Medical Fellows Program (ANT), Alpha Omega Alpha

Carolyn Kuckein Student Research Fellowship to (ANT), a UCSF Breakthrough Grant (E.C.H.), NIH R01AR066735 and R01AR073015 (E.C.H.), a FOP Developmental Grants Program from the Center for Research in FOP & Related Disorders, University of Pennsylvania (E.C.H.), and a California Institute of Regenerative Medicine Bridges 2.0 grant to San Francisco State University (EDUC2-08391, supporting S.H.).

Author Contributions: X. Yu, A.N. Ton, B.M. Morales, J. Chen, and E.C. Hsiao designed the research studies. X. Yu, A.N. Ton, B.M. Morales, Z. Niu, J. Chen, J. Braz, E. Barruet, HJ, K. Cheung, K. Wentworth, S. Hansberry, S. Ali, and I. Nikolli conducted the experiments and acquired data. X. Yu, A.N. Ton, B.M. Morales, J. Chen, M.H. Lai, K. Wentworth, and E.C. Hsiao analyzed the data. E.C. Hsiao, X. Yu, T. Chan, K. Bigay, and J. Ho enrolled patients. X. Yu, A. Kriegstein, A. Basbaum, and E.C. Hsiao wrote the manuscript.

All data and analyses are available in the manuscript or supplementary materials (available at http://links.lww.com/PAIN/B626).

Appendix A. Supplemental digital content

Supplemental digital content associated with this article can be found online at http://links.lww.com/PAIN/B626.

Article history:
Received 15 August 2021
Received in revised form 1 March 2022
Accepted 8 April 2022
Available online 20 April 2022

References

[1] Barruet E, Morales BM, Cain CJ, Ton AN, Wentworth KL, Chan TV, Moody TA, Haks MC, Ottenhoff TH, Hellman J, Nakamura MC, Hsiao EC. NF-kappaB/MAPK activation underlies ACVR1-mediated inflammation in human heterotopic ossification. JCI Insight 2018;3.

[2] Basbaum AI, Bautista DM, Scherrer G, Julius D. Cellular and molecular mechanisms of pain. Cell 2009;139:267–84.

[3] Bautista DM, Pellegrino M, Tsunozaki M. TRPA1: a gatekeeper for inflammation. Annu Rev Physiol 2013;75:181–200.

[4] Bennett DL, Clark AJ, Huang J, Waxman SG, Dib-Hajj SD. The role of voltage-gated sodium channels in pain signaling. Physiol Rev 2019;99:1079–151.

[5] Blankenburg M, Boekens H, Hechler T, Maier C, Krumova E, Scherens A, Magerl W, Aksu F, Zernikow B. Reference values for quantitative sensory testing in children and adolescents: developmental and gender differences of somatosensory perception. PAIN 2010;149:76–88.

[6] Borsook D, Hargreaves R, Bountra C, Porreca F. Lost but making progress-Where will new analgesic drugs come from? Sci Transl Med 2014;6:249sr243.

[7] Buczkowicz P, Hoeman C, Rakopoulos P, Pajovic S, Letourneau L, Dzamba M, Morrison A, Lewis P, Bouffet E, Bartels U, Zuccaro J, Agnihotri S, Ryall S, Barszczyk M, Chornenkyy Y, Bourgey M, Bourque G, Montpetit A, Cordero F, Castelo-Branco P, Mangerel J, Tabori U, Ho KC, Huang A, Taylor KR, Mackay A, Bendel AE, Nazarian J, Fangusaro JR, Karajannis MA, Zagzag D, Foreman NK, Donson A, Hegert JV, Smith A, Chan J, Lafay-Cousin L, Dunn S, Hukin J, Dunham C, Scheinemann K, Michaud J, Zelcer S, Ramsay D, Cain J, Brennan C, Souweidane MM, Jones C, Allis CD, Brudno M, Becher O, Hawkins C. Genomic analysis of diffuse intrinsic pontine gliomas identifies three molecular subgroups and recurrent activating ACVR1 mutations. Nat Genet 2014;46:451–6.

[8] Burnett SH, Kershen EJ, Zhang J, Zeng L, Straley SC, Kaplan AM, Cohen DA. Conditional macrophage ablation in transgenic mice expressing a Fas-based suicide gene. J Leukoc Biol 2004;75:612–23.

[9] Calvo M, Dawes JM, Bennett DL. The role of the immune system in the generation of neuropathic pain. Lancet Neurol 2012;11:629–42.

[10] Cao L, McDonnell A, Nitzsche A, Alexandrou A, Saintot PP, Loucif AJ, Brown AR, Young G, Mis M, Randall A, Waxman SG, Stanley P, Kirby S, Tarabar S, Gutteridge A, Butt R, McKernan RM, Whiting P, Ali Z, Bilsland J, Stevens EB. Pharmacological reversal of a pain phenotype in iPSC-derived sensory neurons and patients with inherited erythromelalgia. Sci Transl Med 2016;8:335ra356.

[11] Cella D, Riley W, Stone A, Rothrock N, Reeve B, Yount S, Amtmann D, Bode R, Buysse D, Choi S, Cook K, Devellis R, DeWalt D, Fries JF, Gershon R, Hahn EA, Lai JS, Pilkonis P, Revicki D, Rose M, Weinfurt K, Hays R, Group PC. The Patient-Reported Outcomes Measurement Information System (PROMIS) developed and tested its first wave of adult self-reported health outcome item banks: 2005-2008. J Clin Epidemiol 2010;63:1179–94.

[12] Chambers SM, Fasano CA, Papapetrou EP, Tomishima M, Sadelain M, Studer L. Highly efficient neural conversion of human ES and iPS cells by dual inhibition of SMAD signaling. Nat Biotechnol 2009;27:275–80.

[13] Chambers SM, Qi Y, Mica Y, Lee G, Zhang XJ, Niu L, Bilsland J, Cao L, Stevens E, Whiting P, Shi SH, Studer L. Combined small-molecule inhibition accelerates developmental timing and converts human pluripotent stem cells into nociceptors. Nat Biotechnol 2012;30:715–20.

[14] Chandran V, Coppola G, Nawabi H, Omura T, Versano R, Huebner EA, Zhang A, Costigan M, Yekkirala A, Barrett L, Blesch A, Michaelevski I, Davis-Turak J, Gao F, Langfelder P, Horvath S, He Z, Benowitz L, Fainzilber M, Tuszynski M, Woolf CJ, Geschwind DH. A systems-level analysis of the peripheral nerve intrinsic axonal growth Program. Neuron 2016;89:956–70.

[15] Descalzi G, Ikegami D, Ushijima T, Nestler EJ, Zachariou V, Narita M. Epigenetic mechanisms of chronic pain. Trends Neurosci 2015;38:237–46.

[16] DiBonaventura MD, Sadosky A, Concialdi K, Hopps M, Kudel I, Parsons B, Cappelleri JC, Hlavacek P, Alexander AH, Stacey BR, Markman JD, Farrar JT. The prevalence of probable neuropathic pain in the US: results from a multimodal general-population health survey. J Pain Res 2017;10:2525–38.

[17] Follansbee TL, Gjelsvik KJ, Brann CL, McParland AL, Longhurst CA, Galko MJ, Ganter GK. Drosophila nociceptive sensitization requires BMP signaling via the canonical SMAD pathway. J Neurosci 2017;37:8524–33.

[18] Fontebasso AM, Papillon-Cavanagh S, Schwartzentruber J, Nikbakht H, Gerges N, Fiset PO, Bechet D, Faury D, De Jay N, Ramkissoon LA, Corcoran A, Jones DT, Sturm D, Johann P, Tomita T, Goldman S, Nagib M, Bendel A, Goumnerova L, Bowers DC, Leonard JR, Rubin JB, Alden T, Browd S, Geyer JR, Leary S, Jallo G, Cohen K, Gupta N, Prados MD, Carret AS, Ellezam B, Crevier L, Klekner A, Bognar L, Hauser P, Garami M, Myseros J, Dong Z, Siegel PM, Malkin H, Ligon AH, Albrecht S, Pfister SM, Ligon KL, Majewski J, Jabado N, Kieran MW. Recurrent somatic mutations in ACVR1 in pediatric midline high-grade astrocytoma. Nat Genet 2014;46:462–6.

[19] Fortin J, Tian R, Zarrabi I, Hill G, Williams E, Sanchez-Duffhues G, Thorikay M, Ramachandran P, Siddaway R, Wong JF, Wu A, Apuzzo LN, Haight J, You-Ten A, Snow BE, Wakeham A, Goldhamer DJ, Schramek D, Bullock AN, Dijke PT, Hawkins C, Mak TW. Mutant ACVR1 arrests glial cell differentiation to drive tumorigenesis in pediatric gliomas. Cancer Cell 2020;37:308–23 e312.

[20] Haanpaa M, Attal N, Backonja M, Baron R, Bennett M, Bouhassira D, Cruccu G, Hansson P, Haythornthwaite JA, Iannetti GD, Jensen TS, Kauppila T, Nurmikko TJ, Rice AS, Rowbotham M, Serra J, Sommer C, Smith BH, Treede RD. NeuPSIG guidelines on neuropathic pain assessment. PAIN 2011;152:14–27.

[21] Hansson P, Backonja M, Bouhassira D. Usefulness and limitations of quantitative sensory testing: clinical and research application in neuropathic pain states. Pain 2007;129:256–9.

[22] Hatsell SJ, Idone V, Wolken DM, Huang L, Kim HJ, Wang L, Wen X, Nannuru KC, Jimenez J, Xie L, Das N, Makhoul G, Chernomorsky R, D'Ambrosio D, Corpina RA, Schoenherr CJ, Feeley K, Yu PB, Yancopoulos GD, Murphy AJ, Economides AN. ACVR1R206H receptor mutation causes fibrodysplasia ossificans progressiva by imparting responsiveness to activin A. Sci Transl Med 2015;7:303ra137.

[23] Hays RD, Bjorner JB, Revicki DA, Spritzer KL, Cella D. Development of physical and mental health summary scores from the patient-reported outcomes measurement information system (PROMIS) global items. Qual Life Res 2009;18:873–80.

[24] Hino K, Ikeya M, Horigome K, Matsumoto Y, Ebise H, Nishio M, Sekiguchi K, Shibata M, Nagata S, Matsuda S, Toguchida J. Neofunction of ACVR1 in fibrodysplasia ossificans progressiva. Proc Natl Acad Sci U S A 2015;112:15438–43.

[25] Hocking LJ, Generation S, Morris AD, Dominiczak AF, Porteous DJ, Smith BH. Heritability of chronic pain in 2195 extended families. Eur J Pain 2012;16:1053–63.

[26] Hoeman CM, Cordero FJ, Hu G, Misuraca K, Romero MM, Cardona HJ, Nazarian J, Hashizume R, McLendon R, Yu P, Procissi D, Gadd S, Becher

OJ. ACVR1 R206H cooperates with H3.1K27M in promoting diffuse intrinsic pontine glioma pathogenesis. Nat Commun 2019;10:1023.
[27] Ji RR, Chamessian A, Zhang YQ. Pain regulation by non-neuronal cells and inflammation. Science 2016;354:572–7.
[28] Kan L, Kitterman JA, Procissi D, Chakkalakal S, Peng CY, McGuire TL, Goldsby RE, Pignolo RJ, Shore EM, Kaplan FS, Kessler JA. CNS demyelination in fibrodysplasia ossificans progressiva. J Neurol 2012; 259:2644–55.
[29] Kan L, Lounev VY, Pignolo RJ, Duan L, Liu Y, Stock SR, McGuire TL, Lu B, Gerard NP, Shore EM, Kaplan FS, Kessler JA. Substance P signaling mediates BMP-dependent heterotopic ossification. J Cell Biochem 2011; 112:2759–72.
[30] Kan L, Mutso AA, McGuire TL, Apkarian AV, Kessler JA. Opioid signaling in mast cells regulates injury responses associated with heterotopic ossification. Inflamm Res 2014;63:207–15.
[31] Kaplan FS, Al Mukaddam M, Pignolo RJ. A cumulative analogue joint involvement scale (CAJIS) for fibrodysplasia ossificans progressiva (FOP). Bone 2017;101:123–8.
[32] Kavelaars A, Heijnen CJ. Immune regulation of pain: friend and foe. Sci Transl Med 2021;13:eabj7152.
[33] Khan F, Yu X, Hsiao EC. Cardiopulmonary and neurologic dysfunctions in fibrodysplasia ossificans progressiva. Biomedicines 2021;9.
[34] Kim BY, Jeong S, Lee SY, Lee SM, Gweon EJ, Ahn H, Kim J, Chung SK. Concurrent progress of reprogramming and gene correction to overcome therapeutic limitation of mutant ALK2-iPSC. Exp Mol Med 2016;48:e237.
[35] Kitterman JA, Strober JB, Kan L, Rocke DM, Cali A, Peeper J, Snow J, Delai PL, Morhart R, Pignolo RJ, Shore EM, Kaplan FS. Neurological symptoms in individuals with fibrodysplasia ossificans progressiva. J Neurol 2012;259:2636–43.
[36] Knaul FM, Farmer PE, Krakauer EL, De Lima L, Bhadelia A, Jiang Kwete X, Arreola-Ornelas H, Gomez-Dantes O, Rodriguez NM, Alleyne GAO, Connor SR, Hunter DJ, Lohman D, Radbruch L, Del Rocio Saenz Madrigal M, Atun R, Foley KM, Frenk J, Jamison DT, Rajagopal MR. Lancet Commission on Palliative C, Pain Relief Study G. Alleviating the access abyss in palliative care and pain relief-an imperative of universal health coverage: the Lancet Commission report. Lancet 2018;391: 1391–454.
[37] Kwan KY, Allchorne AJ, Vollrath MA, Christensen AP, Zhang DS, Woolf CJ, Corey DP. TRPA1 contributes to cold, mechanical, and chemical nociception but is not essential for hair-cell transduction. Neuron 2006; 50:277–89.
[38] Kwan KY, Glazer JM, Corey DP, Rice FL, Stucky CL. TRPA1 modulates mechanotransduction in cutaneous sensory neurons. J Neurosci 2009; 29:4808–19.
[39] Lin I, Wiles L, Waller R, Goucke R, Nagree Y, Gibberd M, Straker L, Maher CG, O'Sullivan PPB. What does best practice care for musculoskeletal pain look like? Eleven consistent recommendations from high-quality clinical practice guidelines: systematic review. Br J Sports Med 2020;54: 79–86.
[40] Liu L, Zhu Y, Noe M, Li Q, Pasricha PJ. Neuronal transforming growth factor beta signaling via SMAD3 contributes to pain in animal models of chronic pancreatitis. Gastroenterology 2018;154:2252–65.e2252.
[41] Livak KJ, Schmittgen TD. Analysis of relative gene expression data using real-time quantitative PCR and the 2(-Delta Delta C(T)) Method. Methods 2001;25:402–8.
[42] Magerl W, Krumova EK, Baron R, Tolle T, Treede RD, Maier C. Reference data for quantitative sensory testing (QST): refined stratification for age and a novel method for statistical comparison of group data. PAIN 2010; 151:598–605.
[43] Mantick N, Bachman E, Baujat G, Brown M, Collins O, De Cunto C, Delai P, Eekhoff M, Zum Felde R, Grogan DR, Haga N, Hsiao E, Kantanie S, Kaplan F, Keen R, Milosevic J, Morhart R, Pignolo R, Qian X, di Rocco M, Scott C, Sherman A, Wallace M, Williams N, Zhang K, Bogard B. The FOP connection registry: design of an international patient-sponsored registry for fibrodysplasia ossificans progressiva. Bone 2018;109:285–90.
[44] Matsumoto Y, Hayashi Y, Schlieve CR, Ikeya M, Kim H, Nguyen TD, Sami S, Baba S, Barruet E, Nasu A, Asaka I, Otsuka T, Yamanaka S, Conklin BR, Toguchida J, Hsiao EC. Induced pluripotent stem cells from patients with human fibrodysplasia ossificans progressiva show increased mineralization and cartilage formation. Orphanet J Rare Dis 2013;8:190.
[45] Matsuo K, Lepinski A, Chavez RD, Barruet E, Pereira A, Moody TA, Ton AN, Sharma A, Hellman J, Tomoda K, Nakamura MC, Hsiao EC. ACVR1(R206H) extends inflammatory responses in human induced pluripotent stem cell-derived macrophages. Bone 2021:116129.
[46] McDermott LA, Weir GA, Themistocleous AC, Segerdahl AR, Blesneac I, Baskozos G, Clark AJ, Millar V, Peck LJ, Ebner D, Tracey I, Serra J, Bennett DL. Defining the functional role of NaV1.7 in human nociception. Neuron 2019;101:905–19 e908.
[47] Miyaoka Y, Chan AH, Judge LM, Yoo J, Huang M, Nguyen TD, Lizarraga PP, So PL, Conklin BR. Isolation of single-base genome-edited human iPS cells without antibiotic selection. Nat Methods 2014;11:291–3.
[48] Mogil JS. Animal models of pain: progress and challenges. Nat Rev Neurosci 2009;10:283–94.
[49] Mohedas AH, Wang Y, Sanvitale CE, Canning P, Choi S, Xing X, Bullock AN, Cuny GD, Yu PB. Structure-activity relationship of 3,5-diaryl-2-aminopyridine ALK2 inhibitors reveals unaltered binding affinity for fibrodysplasia ossificans progressiva causing mutants. J Med Chem 2014;57:7900–15.
[50] Nickolls AR, Lee MM, Espinoza DF, Szczot M, Lam RM, Wang Q, Beers J, Zou J, Nguyen MQ, Solinski HJ, AlJanahi AA, Johnson KR, Ward ME, Chesler AT, Bonnemann CG. Transcriptional programming of human mechanosensory neuron subtypes from pluripotent stem cells. Cell Rep 2020;30:932–46 e937.
[51] Parikh P, Hao Y, Hosseinkhani M, Patil SB, Huntley GW, Tessier-Lavigne M, Zou H. Regeneration of axons in injured spinal cord by activation of bone morphogenetic protein/Smad1 signaling pathway in adult neurons. Proc Natl Acad Sci U S A 2011;108:E99–107.
[52] Percie du Sert N, Rice AS. Improving the translation of analgesic drugs to the clinic: animal models of neuropathic pain. Br J Pharmacol 2014;171: 2951–63.
[53] Pignolo RJ, Bedford-Gay C, Liljesthrom M, Durbin-Johnson BP, Shore EM, Rocke DM, Kaplan FS. The natural history of flare-ups in fibrodysplasia ossificans progressiva (FOP): a comprehensive global assessment. J Bone Miner Res 2016;31:650–6.
[54] Pignolo RJ, Shore EM, Kaplan FS. Fibrodysplasia ossificans progressiva: clinical and genetic aspects. Orphanet J Rare Dis 2011;6:80.
[55] Price TJ, Flores CM. Critical evaluation of the colocalization between calcitonin gene-related peptide, substance P, transient receptor potential vanilloid subfamily type 1 immunoreactivities, and isolectin B4 binding in primary afferent neurons of the rat and mouse. J Pain 2007;8:263–72.
[56] Ramachandran A, Vizan P, Das D, Chakravarty P, Vogt J, Rogers KW, Muller P, Hinck AP, Sapkota GP, Hill CS. TGF-beta uses a novel mode of receptor activation to phosphorylate SMAD1/5 and induce epithelial-to-mesenchymal transition. Elife 2018;7.
[57] Renthal W, Tochitsky I, Yang L, Cheng YC, Li E, Kawaguchi R, Geschwind DH, Woolf CJ. Transcriptional reprogramming of distinct peripheral sensory neuron subtypes after axonal injury. Neuron 2020. 108:128–144.
[58] Rolke R, Baron R, Maier C, Tolle TR, Treede RD, Beyer A, Binder A, Birbaumer N, Birklein F, Botefur IC, Braune S, Flor H, Huge V, Klug R, Landwehrmeyer GB, Magerl W, Maihofner C, Rolko C, Schaub C, Scherens A, Sprenger T, Valet M, Wasserka B. Quantitative sensory testing in the German Research Network on Neuropathic Pain (DFNS): standardized protocol and reference values. PAIN 2006;123:231–43.
[59] Saijilafu HEM, Liu CM, Jiao Z, Xu WL, Zhou FQ. PI3K-GSK3 signalling regulates mammalian axon regeneration by inducing the expression of Smad1. Nat Commun 2013;4:2690.
[60] Seltzer Z, Dubner R, Shir Y. A novel behavioral model of neuropathic pain disorders produced in rats by partial sciatic nerve injury. PAIN 1990;43: 205–18.
[61] Shields SD, Eckert WA III, Basbaum AI. Spared nerve injury model of neuropathic pain in the mouse: a behavioral and anatomic analysis. J Pain 2003;4:465–70.
[62] Shiers S, Klein RM, Price TJ. Quantitative differences in neuronal subpopulations between mouse and human dorsal root ganglia demonstrated with RNAscope in situ hybridization. PAIN 2020;161: 2410–24.
[63] Shiers SI, Sankaranarayanan I, Jeevakumar V, Cervantes A, Reese JC, Price TJ. Convergence of peptidergic and non-peptidergic protein markers in the human dorsal root ganglion and spinal dorsal horn. J Comp Neurol 2021;529:2771–88.
[64] Shore EM, Xu M, Feldman GJ, Fenstermacher DA, Cho TJ, Choi IH, Connor JM, Delai P, Glaser DL, LeMerrer M, Morhart R, Rogers JG, Smith R, Triffitt JT, Urtizberea JA, Zasloff M, Brown MA, Kaplan FS. A recurrent mutation in the BMP type I receptor ACVR1 causes inherited and sporadic fibrodysplasia ossificans progressiva. Nat Genet 2006;38: 525–7.
[65] Spira ME, Hai A. Multi-electrode array technologies for neuroscience and cardiology. Nat Nanotechnol 2013;8:83–94.
[66] Takahashi K, Tanabe K, Ohnuki M, Narita M, Ichisaka T, Tomoda K, Yamanaka S. Induction of pluripotent stem cells from adult human fibroblasts by defined factors. Cell 2007;131:861–72.
[67] Talavera K, Startek JB, Alvarez-Collazo J, Boonen B, Alpizar YA, Sanchez A, Naert R, Nilius B. Mammalian transient receptor potential TRPA1 channels: from structure to disease. Physiol Rev 2020;100: 725–803.

[68] Tavares-Ferreira D, Shiers S, Ray PR, Wangzhou A, Jeevakumar V, Sankaranarayanan I, Cervantes AM, Reese JC, Chamessian A, Copits BA, Dougherty PM, Gereau RWT, Burton MD, Dussor G, Price TJ. Spatial transcriptomics of dorsal root ganglia identifies molecular signatures of human nociceptors. Sci Transl Med 2022;14:eabj8186.
[69] Taylor KR, Mackay A, Truffaux N, Butterfield Y, Morozova O, Philippe C, Castel D, Grasso CS, Vinci M, Carvalho D, Carcaboso AM, de Torres C, Cruz O, Mora J, Entz-Werle N, Ingram WJ, Monje M, Hargrave D, Bullock AN, Puget S, Yip S, Jones C, Grill J. Recurrent activating ACVR1 mutations in diffuse intrinsic pontine glioma. Nat Genet 2014;46:457–61.
[70] Tramullas M, Lantero A, Diaz A, Morchon N, Merino D, Villar A, Buscher D, Merino R, Hurle JM, Izpisua-Belmonte JC, Hurle MA. BAMBI (bone morphogenetic protein and activin membrane-bound inhibitor) reveals the involvement of the transforming growth factor-beta family in pain modulation. J Neurosci 2010;30:1502–11.
[71] Tsantoulas C, McMahon SB. Opening paths to novel analgesics: the role of potassium channels in chronic pain. Trends Neurosci 2014;37:146–58.
[72] van Hecke O, Austin SK, Khan RA, Smith BH, Torrance N. Neuropathic pain in the general population: a systematic review of epidemiological studies. PAIN 2014;155:654–62.
[73] Wainger BJ, Buttermore ED, Oliveira JT, Mellin C, Lee S, Saber WA, Wang AJ, Ichida JK, Chiu IM, Barrett L, Huebner EA, Bilgin C, Tsujimoto N, Brenneis C, Kapur K, Rubin LL, Eggan K, Woolf CJ. Modeling pain in vitro using nociceptor neurons reprogrammed from fibroblasts. Nat Neurosci 2015;18:17–24.
[74] Walco GA, Dworkin RH, Krane EJ, LeBel AA, Treede RD. Neuropathic pain in children: special considerations. Mayo Clin Proc 2010;85(3 suppl):S33–41.
[75] Woolf CJ, Bennett GJ, Doherty M, Dubner R, Kidd B, Koltzenburg M, Lipton R, Loeser JD, Payne R, Torebjork E. Towards a mechanism-based classification of pain? PAIN 1998;77:227–9.
[76] Wu T, Chen SS. Differential diagnosis between fibrodysplasia ossificans progressiva and childhood dermatomyositis with calcinosis. J Formos Med Assoc 1993;92:569–76.
[77] Xu P, Van Slambrouck C, Berti-Mattera L, Hall AK. Activin induces tactile allodynia and increases calcitonin gene-related peptide after peripheral inflammation. J Neurosci 2005;25:9227–35.
[78] Yezierski RP, Hansson P. Inflammatory and neuropathic pain from bench to bedside: what went wrong? J Pain 2018;19:571–88.
[79] Yu PB, Deng DY, Lai CS, Hong CC, Cuny GD, Bouxsein ML, Hong DW, McManus PM, Katagiri T, Sachidanandan C, Kamiya N, Fukuda T, Mishina Y, Peterson RT, Bloch KD. BMP type I receptor inhibition reduces heterotopic [corrected] ossification. Nat Med 2008;14:1363–9.
[80] Yu X, Liu H, Hamel KA, Morvan MG, Yu S, Leff J, Guan Z, Braz JM, Basbaum AI. Dorsal root ganglion macrophages contribute to both the initiation and persistence of neuropathic pain. Nat Commun 2020;11:264.
[81] Zhu W, Xu P, Cuascut FX, Hall AK, Oxford GS. Activin acutely sensitizes dorsal root ganglion neurons and induces hyperalgesia via PKC-mediated potentiation of transient receptor potential vanilloid I. J Neurosci 2007;27:13770–80.
[82] Zhu Y, Colak T, Shenoy M, Liu L, Mehta K, Pai R, Zou B, Xie XS, Pasricha PJ. Transforming growth factor beta induces sensory neuronal hyperexcitability, and contributes to pancreatic pain and hyperalgesia in rats with chronic pancreatitis. Mol Pain 2012;8:65.